T. C.
SELÇUK UNIVERSITY
GRADUATE SCHOOL OF NATURAL SCIENCES

DETECTION OF IMPERFECTIONS IN NON-METAL SEWER PIPES BY IMAGE PROCESSING

MOHAMMED QAYS JAMEEL AL-SALIHI

MASTER'S THESIS

Computer Engineering Department

January - 2018
KONYA

TEZ KABUL VE ONAYI

Mohammed Qays Jameel AL-SALIHI tarafından hazırlanan "METAL OLMAYAN KANALİZASYON BORULARINDAKİ KUSURLARIN GÖRÜNTÜ İŞLEME YOLUYLA TESPİTİ" adlı tez çalışması 11/01/2018 tarihinde aşağıdaki jüri tarafından oy birliği ile Selçuk Üniversitesi Fen Bilimleri Enstitüsü Bilgisayar Mühendisliği Anabilim Dalı'nda YÜKSEK LİSANS TEZİ olarak kabul edilmiştir.

Jüri Üyeleri	**İmza**
Başkan	
Yrd.Doç.Dr. Onur İNAN	....
Danışman	
Yrd.Doç.Dr. Murat SELEK	....
Üye	
Yrd.Doç.Dr. Ahmet BABALIK	....

Yukarıdaki sonucu onaylarım.

Prof. Dr. Mustafa YILMAZ
FBE Müdürü

TEZ BİLDİRİMİ

Bu tezdeki bütün bilgilerin etik davranış ve akademik kurallar çerçevesinde elde edildiğini ve tez yazım kurallarına uygun olarak hazırlanan bu çalışmada bana ait olmayan her türlü ifade ve bilginin kaynağına eksiksiz atıf yapıldığını bildiririm.

DECLARATION

I hereby declare that all information in this document has been obtained and presented in accordance with academic rules and ethical conduct. I also declare that, as required by these rules and conduct, I have fully cited and referenced all material and results that are not original to this work.

Mohammed Qays Jameel AL-SALIHI

Date 11/01/2018

ÖZET

YÜKSEK LİSANS TEZİ

METAL OLMAYAN KANALİZASYON BORULARINDAKİ KUSURLARIN GÖRÜNTÜ İŞLEME YOLUYLA TESPİTİ

Mohammed Qays Jameel AL-SALIHI

Selçuk Üniversitesi Fen Bilimleri Enstitüsü
Bilgisayar Mühendisliği Anabilim Dalı

Danışman: Yrd.Doç.Dr. Murat SELEK

2018, 65 Sayfa

Jüri

Yrd.Doç.Dr. Onur İNAN
Yrd.Doç.Dr. Murat SELEK
Yrd.Doç.Dr. Ahmet BABALIK

Bu çalışmada, görüntü işleme metotları kullanılarak operatör olmaksızın yeni yapılmış bir kanalizasyon kanalının sağlamlık kontrolünü gerçekleştirebilen bir yöntem geliştirilmiştir. Çalışma, yaygın olarak kullanılan metal olmayan (beton) kanalizasyon kanalları üzerinde gerçekleştirilmiştir. Bu yöntem ile yapımı bitmiş fakat daha hizmete alınmamış kanalizasyon kanallarının sağlamlık kontrolünün yapılabilmesi hedeflenmiştir.

Çalışmamızda yapımı tamamlanmış fakat hizmete alınmamış olan kanalların içini gösteren video görüntüleri kullanılmıştır. Çalışmada kullanılan kanal içi görüntüler belediye tarafından kontrol için yetkilendirilmiş olan TENOM YAPI MADENCİLİK ŞTİ.'nden temin edilmiştir.

Elde edilen görüntüler kullanılarak, kanalizasyon kanallarında yaygın olarak görülen ek açıklığı, mil, atık ve kılcal çatlaktan oluşan 4 kusurun görüntü işleme yoluyla tespiti yapılmaya çalışılmıştır. Bunun için öncelikle görüntüler Sobel operator, Prewitt operator, Robert's Cross operator, Canny operator, Median gibi filtreler kullanılarak gürültü yok etme, yumuşatma, kenar artırma özelliklerini geliştirmek için filtre edilmiştir. Daha sonra ise görüntüden özellik çıkarabilmek için K-ortalama kümeleme, kenar tespiti, renk uzayı tabanlı bölütleme, görüntü bölütleme olmak üzere 4 farklı algoritma kullanılmıştır. Son olarak görüntüden elde edilen özellikleri kullanarak mil, ek açıklığı, atık ve kılcal çatlak olarak ifade ettiğimiz kusurları tespit edebilen MATLAB kodları geliştirilmiştir. Geliştirilen kodlar kullanılarak Matlab ortamında bir grafik arayüz tasarlanmış ve elde edilen sonuçlar bu arayüz üzerinden kullanıcıya sunulmuştur. Aynı zamanda sonuçların bir rapor şeklinde kullanıcıya sunulması sağlanmıştır. Elde edilen sonuçlar, geliştirilen özellik çıkarma yönteminin metal olmayan kanalizasyon borularında meydana gelen mil, atık, ek açıklığı ve kılcal çatlak kusurlarını yüksek bir başarı ile tespit edebildiğini ortaya koymaktadır.

Anahtar Kelimeler: K-ortalama kümeleme, Kenar tespiti, Renk uzayı tabanlı bölütleme ve Görüntü bölütleme.

ABSTRACT

MASTER'S THESIS

DETECTION OF IMPERFECTIONS IN NON-METAL SEWER PIPES BY IMAGE PROCESSING

Mohammed Qays Jameel AL-SALIHI

THE GRADUATE SCHOOL OF NATURAL AND APPLIED SCIENCE OF SELÇUK UNIVERSITY
THE DEGREE OF MASTER OF SCIENCE
IN COMPUTER ENGINEERING

Advisor: Assist. Prof. Murat SELEK

2018, 65 Pages

Jury

Asst.Prof.Dr. Onur İNAN
Asst.Prof.Dr. Murat SELEK
Asst.Prof.Dr. Ahmet BABALIK

In this work, a method was developed to detect any defect in a newly constructed sewer channel without using an operator by using image processing methods. The study was carried out on non-metal sewer pipes used commonly. This method is aimed to control the defect of sewer pipes which are finished but not used yet.

In our work, video images that show the inside of sewer pipes which were completed but not yet serviced were used. In pipes' images used in this study were obtained from the TENOM CONSTRUCTION MINING COMPANY authorized by the municipality for control.

Using the obtained images, 4 defects that are common in sewe pipes, such as impurities, additional aperture, residues and capillary fraction, were tried to be detected by image processing. First, images were filtered to reduece noises, smoothing, edge enhancement by using filters such as Sobel operator, Prewitt operator, Robert's Cross operator, Canny operator, Median. Then, four different algorithms were applied to extract feature from the image: K-mean clustering, edge detection, color space based segmentation, and image segmentation. Finally, MATLAB codes have been developed to detect defects, that are expressed as impurities, additional aperture, residues and capillary fraction, using the features obtained from the image. A graphical interface was designed in MATLAB environment using the developed codes and the results are presented to the user through this interface. At the same time, the results were presented to the user in the form of a report. The obtained results show that the purposed method can detect the defects such as the impurities, residues, additional aperture and capillary fractions in the non-metal sewer pipes with a high success rate.

Keywords: K-means clustering, Edge detection, Segment based on color space and Image segmentation.

ÖNSÖZ

Yüksek Lisans Tez çalışmalarım esnasında her konuda yardımlarını esirgemeyen kıymetli hocam Yrd.Doç.Dr. Murat SELEK'e teşekkürlerimi sunarım. Bunun yanında çalışmamızda verilerini kullanmamıza izin veren TENOM YAPI MEDENCİLİK Şti'den Oğuz ŞIH'a ve çalışmalarım boyunca vermiş oldukları destekten dolayı aileme teşekkür ederim.

ACKNOWLEDGMENT

I take this opportunity to express with pleasure my deep gratitude to my supervisor Assist. Prof. Dr. Murat SELEK for his assistance, scientific support, kindness and the precious directions and time devoted to take my hand during my M.Sc. work and preparing this thesis. Thanks also are due to the TENOM CONSTRUCTION MINING company that provided us with datasets required in this study. I also eagerly wish to convey a lovely greetings and thanks to my beloved family who supported me by all means and enable me to conduct this work successfully.

Mohammed Qays Jameel AL-SALIHI
KONYA-2018

CONTENTS

LIST OF FIGURES

LIST OF TABLE

TERMS AND ACRONYMS

PR	: Photographic Reproduction
EDT	: Easter Daylight Time
CAT	: Computerized Axial Tomography
CT	: Computerized Tomography
IP	: Image Processing
SPD	: Spectrum Power Distribution
NTSC	: National Television Standard Committee
CI	: Color Information
HSV	: Hue Saturation Value
HIS	: Hue Saturation Intensity
MFL	: Magnetic Flux Leakage
EMAT	: Electromagnetic Acoustic Transducer
RFDC	: Remote Field Eddy Current
SSET	: Sewer Scanner and Evaluation Technology
ST	: Smoke Testing
LDT	: Leak Defectors Technique
GPR	: Ground Penetrating Radar
SO	: Sobel Operator
PO	: Prewitt Operator
CO	: Canny Operator
MF	: Median Filter
NDT	: Non-Destructive Testing
LLL	: Lambda Locked Loop
BPN	: Back Propagation Neural network
SVM	: Support Vector Machine
FET	: Feature Extraction Technique
FE	: Feature Extraction
CF	: Color Feature
ED	: Edge Detection
+ve	: Positive
-ve	: Negative
DCT	: Data Clustering Technique
CCTV	: Closed Circuit Television

GUI **:** Graphic User Interface

1. INTRODUCTION

Image Processing (IP) is a mechanism to improve raw images delivered by photographing devices located on satellites, space probes and airplanes or photographs of our daily activists for different uses; different techniques were invented in IP in the past 40-50 years, by using image of divergent source. IP acquired popularity due to its availability of personal computers, memory devices of wide capacity, graphics software, ets. it can be used in divergent application fields of application like remote sensing, medicine photographing, nondestructive evaluation, forensic experiment, textiles, military, cinema industries, document processing, graphic arts and print industry (Gupta and Kaur, 2014). A known stage in the fields of IP are image scrutiny, storing, boosting and translation. Figure (1.1.) is shown a diagram of image scanner-digitizer.

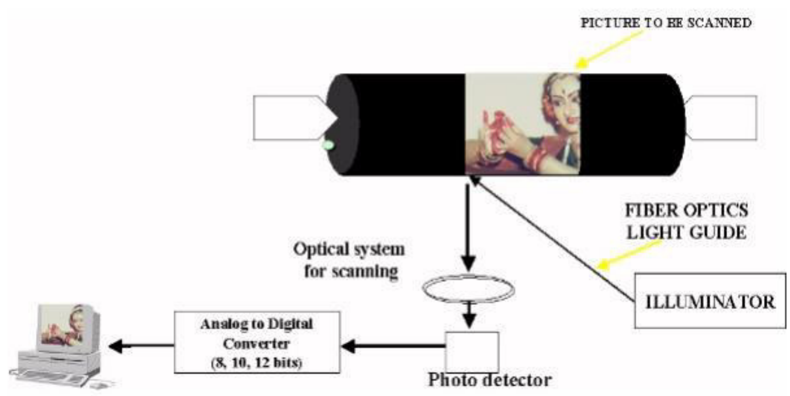

Figure 1.1. Basic Image Processing Technique

Underground of the world cities and roads lie millions of pipes of sewer systems carry away westes, and some of these systems are in a deterioration condition. Maintenance and inspection of defects by human post a major challenge for most of the municipalities. Regular service and defect inspection of the pipelines systems add to life cycle costs and liabilities and in extreme situations causing reduction or even stoppage of services.

Automatic identification of different pipe defects is of substantial importance since it has the potential to solve problems of fatigue, subjectivity, and ambiguity, leading to economic benefits. The main efforts of the research are placed on investigating algorithms and techniques for image pre-processing, segmentation of pipe objects (i.e., cracks, holes, joints, laterals, and collapse surface), crack detection, feature extraction and classification of defects.

Pipeline defect detection systems range from simple, visual inspection to complex inspection systems. No one method is universally applicable and operating requirements dictate which method is the most cost effective. Since the last century, efforts were continued to design and construct non-metal sewer pipeline inspection equipment. Many types of equipment have been developed and are being used in developed countries. Among these equipment CCTV, Ultrasound sensor, and Sonar based systems are used. Some of these systems have not become so popular due to the problems of limited practical applications, affordability and acceptability as well as usefulness.

In sixties, using ultrasound sensors invistigetors found many characteristics of these sensors such as object identification by its resonance. Some proposed Smoke Testing technique, this method has been applied in the 1960s for detecting leakage by injection of smoke in the pipe. Whereas, others introduced a technique for location estimation for continuous outdoor translocation of a robot moves autonomously. This technique was based upon maximum similarity calculation. Data combination procedure was also given.

In the 1999s, also, Thermographic non-destructive testing employing thermo-resistance influence of the defect to inspect the most complexed defects inside any complex pipeline system, was introduced. The device has infrared thermal video for measuring the temperature distribution among the surface of the structure. Fiber optical connection system was good method enable to clear vision and find out the wedded part below the robot while moving for inspection, segested in the same years.

But in 2000s, many workers worked on automated image-based inspection, that aims to extract information from an image on the conditions of objects represented in the image. Usually it is impossible to extract this information concerning the dimensions of objects or their defect properties directly from the image. Basically, all machine vision systems involve image acquisition, image pre-processing, segmentation, and extracting relevant features for classification of the type, severity, and extent of defects present in the image.

The old and traditional methods in pipeline inspection were depending upon using inspectors to be sent into the pipe to check and inspect any possible defect occurrence. By this method, the internal situation inside the pipe was efficiently and accurately determined. Hence, this may cause to man dangerous risk and unhealthy environment. In addition, it is also impractical to be used for some pipeline system. So, new inspection technique has been developed nowadays to deals with this problem, and to substitute the old systems of inspection (Daher, 2015).

The aim of this investigation is to find out accurate and fast detection means of the damages that may occur in the non-metal sewer underground pipelines (i.e. Impurities, Additional aperture, Residues and Capillary fraction (figure 1.2.)). These disorders may be discovered via extracting the characteristic from interior image taken and tackled through suitable filters to improve its appearance and ultimately subjected to feature extraction process to extract and determine their characters, and at last step, finding out and diagnosing the faults and disadvantages may exist in the tested pipelines, through passing the videos into our pre-designed program to get a final report (by ckliking on publish bottun) having all kinds of present defects and time of its occurring in the videos automatically, without the need to the human eye.

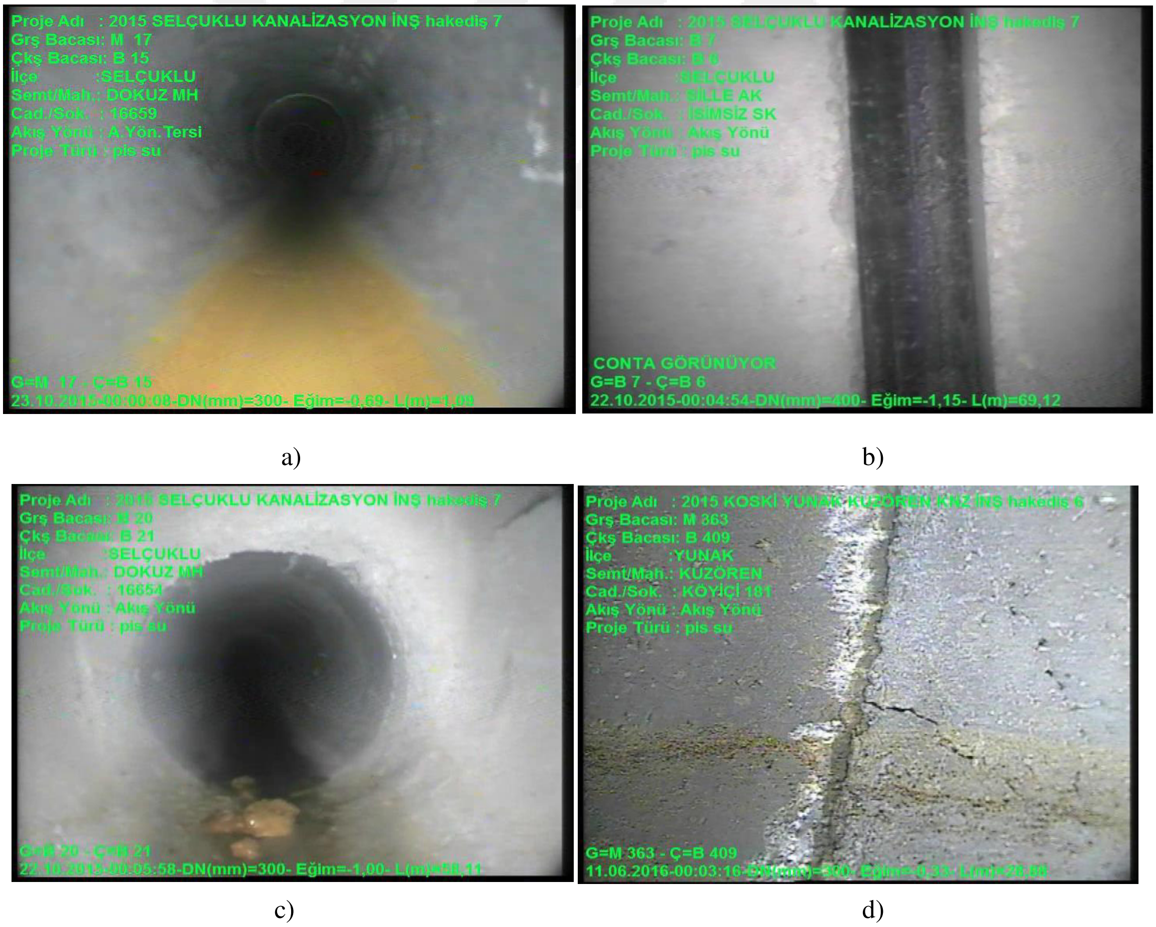

Figure 1.2. Kinds of defects under study a) impurity, b) additional aperture, c) residues and d) capillary fraction

2. LITERATURE REVIEW

Since the beginning of the eighth decade of the last century, efforts were continued to design and construct non-metal sewer pipeline inspection equipment. Many types of equipment have been developed and are being used in developed countries. Among these equipment CCTV, Ultrasound sensor, and sonar based systems are used. Some of these systems have not become so popular due to the problems of limited practical applications, affordability and acceptability as well as usefulness.

2.1 Detect the Leakage

(Magori, 1989) introduced some brilliant ultrasound sensors (some presence detectors) and thermometer Lambda Locked Loop (LLL) flow, and conducted several investigations on these sensors and found many characteristics of these sensors such as object identification by its resonance.

(Allouche and Freure, 2002) proposed Smoke Testing (ST) technique, this method has been applied in the 1960s for detecting leakage by injection of smoke in the pipe. In this method, smoke is injected into the manhole, and after that use a blower to push the smoke through the crack, voids or defects. Leak and defect would be detected when the smoke appears from the pipe segment.

(Feeney et al., 2009) proposed Leak Detectors Technique (LDT), this method is utilized to inspect pipe leakage by diagnosing their noises in pressurized sewer pipe. Its mechanism, however, is estimating the delay in time on the basis of wave speed calculates. Listening rods, underwater microphones, leak noise correlators and in-line devices, are the methods of detecting leakage of pipe.

(Hao et al., 2012) proposed Magnetic Flux Leakage (MFL), in this technique a gauge is inserted into the metallic pipelines. Corrosion can be detected by this method. Also, pitting defects of bad situation can be detected.

(Feng et al., 2016) introduced circumference defects of welding in gas and oil pipes, methods of non-destruction test, and generalized systematic progress in studies on technical principles, the analysis of signals, methods at determine defect size as well as inspection dependability etc. of magnetic flux leakage (MFL) inspection. Also, reported new methods of inspections and gave references for applying of these techniques in defect inspection.

2.2 Image Processing Techniques

(Qin and Bao, 1995) presented Thermographic non-destructive testing (NDT) employing thermo-resistance influence of the defect to inspect the most complexed defects inside any complex pipeline system. The device has infrared thermal video for measuring the temperature distribution among the surface of the structure, a computer with a PIP 1024B image board can conduct image processing for thermographs, as well as a HP inkjet XL printer.

(Duran et al., 2002) reported a detailed method of automatic inspection of defects. This method included many steps starting with segmentation of images into geometrical characters and the location (regions) of the defects. Automatically recognition, assessment, and pipe defects categorization were done by computing of a partial histogram based on adaptive image processing.

(Ohtani and Baba, 2004) introduced a shape recognition system through arrangement of ultrasonic sensor array and CCD image sensors. This technique permits using in cases of difficult to recognize an object shape using ultrasound sensor array alone or CCD image sensor alone.

(Marsland et al., 2005) introduced a substituted method to inspect defects presents in the pipes using novelty detection. A neural network was used to ignore normal conception, that suggested not any problem, therefore, objects that robot did not sense previously was highlighted 18 as a possible error. This decreases the possibility of false negatives. A novelty filter that can be operated on-line was also presented. Hence, every new input was evaluated for novelty regarding the data have been seen.

(Daniels, 2005; Hao et al., 2012) proposed Ground Penetrating Radar (GPR), it is nondestructive technique utilizing electromagnetic waves to detect subsurface materials. Many kinds of GPR are used, such as spatial domain, frequency domain and time domain types. Leak, video, and pipe collapse can be detected by this method.

(Yang and Su, 2008) suggested as a first step using the image processing technique, implicating wavelet transform and computation of co-occurrence matrices, for describing the textures of the pipe defects. Therefore, they adopted three platforms; back-propagation neural network (BPN), radial basis network (RBN) and support vector machine (SVM) to categorize pipe defect format. Results reflected that SVM was the best by given 60% diagnosis accuracy, while Bayesian classifier gave 57.4% diagnosis accuracy.

(Xue-Fei and Hua, 2009) suggested a defect feature extraction algorithm under HSV color space depending upon the image processing. The suggested method able to discover defects from the background, kinds of defects of the underground pipelines could be classified in the estimation steps.

(Gao et al., 2017) proposed an automatic and effective novel methodology for detection and identification the defect in industrial pipelines, is based on image processing. This procedure has three steps. First, conversion the RGB image of the pipelines into a grayscale image. The second is extraction the pipelines and ultimately the detection and identification of the detect.

2.3 CCTV Technique

(Hao et al., 2012) proposed Closed-Circuit Television (CCTV), this technique was first applied in the 1960s for inspection inside the pipelines. In this method, a robot equipped with camera is inserted inside the pipeline from a hole. The robot is controlled by the inspector. By this technique, the inspector can get a lit up image of the defective area from inside of the pipe, does not need the man entry as well as easy to inspect in details by zooming in and out of the area under investigation. On the other hand, some disadvantages are image can only be taken above the water level, image does not contain details about defect dimensions, and it also cannot determine whether a crack extends to the outside surface of the pipe.

(Allouche and Freure, 2002) proposed Sewer Scanner and Evaluation Technology (SSET), this technique was developed to improve CCTV. It is a multi-sensor technique working along the pipe without stopping at every defective area. Therefore, it is more applicable and effective than CCTV. By this method, the test of the defects can be done after the end of the device tour inside the pipeline. This method also, is capable to scan the entire surface of the pipe in 360 degrees, and can inspect horizontal and vertical pipe deflection.

2.4 Laser Technique

(Nassiraei et al., 2007) presented KANTARO, which is the prototype of a passive-active intelligent, completely independent, un-tethered robot with an intelligent unit in its sensor and mode of action. KANTARO, this device has a newly passive-active intelligent mode of action, can move throughout the pipe and passing divergent pipe curvatures easily, without the help of the controller or reading of the sensor. For realizing the mechanism of the action of this device, a macro-intelligent 2D Laser scanner was developed to detect the navigational landmarks, by the computer and in independent manner. This device has fish eye camera to inspect situation and presented detection.

(Safizadeh and Azizzadeh, 2012) introduced a new methodology depending upon the laser generated rings onto the inner wall of the pipelines. Holes and defects locations on the inner wall of the pipelines are detected via analysis of the intensity of the light. Laser intensity is depending upon many factors, like the ring, angle incidence or smoothness of the scattering surface. Unordinary values in one of these factors may result false defect detection. Therefore, it is necessary to hold an enough knowledge of the laser reflectance phenomena for enhancement of the system performance and for realization of its restrictions.

2.5 Different Other Techniques

(Jensen and Svendsen, 1992) proposed a technique based upon fields of pulse pressure fields from ultrasound transducer. The pulsed pressure fields were estimated by Tupholme Stepanishen method. By this method continuously waved and pulse-resonance can also handle. The calculation of the field was by dividing the surface into small rectangles and then summing their response. By using far-field approximation they got fast estimation of the fields.

(Maeyama et al., 1995) introduced a technique for location estimation for continuous outdoor translocation of a robot moves autonomously. This technique was based upon maximum similarity calculation. Data combination procedure was also given.

(Kawaguchi et al., 1995) gave a detailed explanation of a new successful technique, connecting system and vision system of a robot inspecting inside the pipelines, based upon two magnetic wheels. Fiber optical connection system was used for friction reduction. Optical system was made in minimum size, in order to enable it for clear vision and find out the wedded part below the robot while moving for inspection.

(Sinha, 2000) introduces three-steps technique for crack detection, first, D1 and D2 filters were used for extraction the cracks taking into consideration characteristic of pixels in a small vicinity. Secondly, a single respond as well as an associated direction in each pixel. Last stage was the processing of the results by cleaning and relating operations to obtain crack segments.

(Paletta and Pinz, 2000) presented strengthen learning is the context of the detection of the object visually, inclusion of objects identification tasks in corresponding localization framework. They reported that a decision making learns the efficient fusion behavior directly from the interaction with its stochastic environment in a semiconductor loop. The introduced visual detection system works in adaptive and autonomous manner.

3. MATERIALS AND METHODS

3.1. Materials

Underground sewer systems are used widely for big cities, distract and habituated villages. Municipals always responsible for controlling and managing these systems. This type of business is in general given to privet sector for implementation. After constructing the system, it should be tested and delivered. In case of many defects in the system, the company is responsible for manipulating and fixing the defects and hand the system over. Again the system is submitted to another test by an operator trained for this task.

In this study, pipelines are tested and tackled using image processing methods by the images taken from inside the pipelines without the need to the operator. On the other hand, this investigation was conducted on non-metal sewer pipes. Photographing process, however, was done by TENOM YAPI MADENCİLİK, which authorized by the municipals of the Konya city. Figure (3.1.) show the robot having APEX-90 camera used to provide the image required for this study. Figure (3.2.) also imply the detection operation using robot, computer and other tools.

Figure 3.1. Camera and Robot used in photographing inside the pipe

Figure 3.2. Vehicle with photographing operation

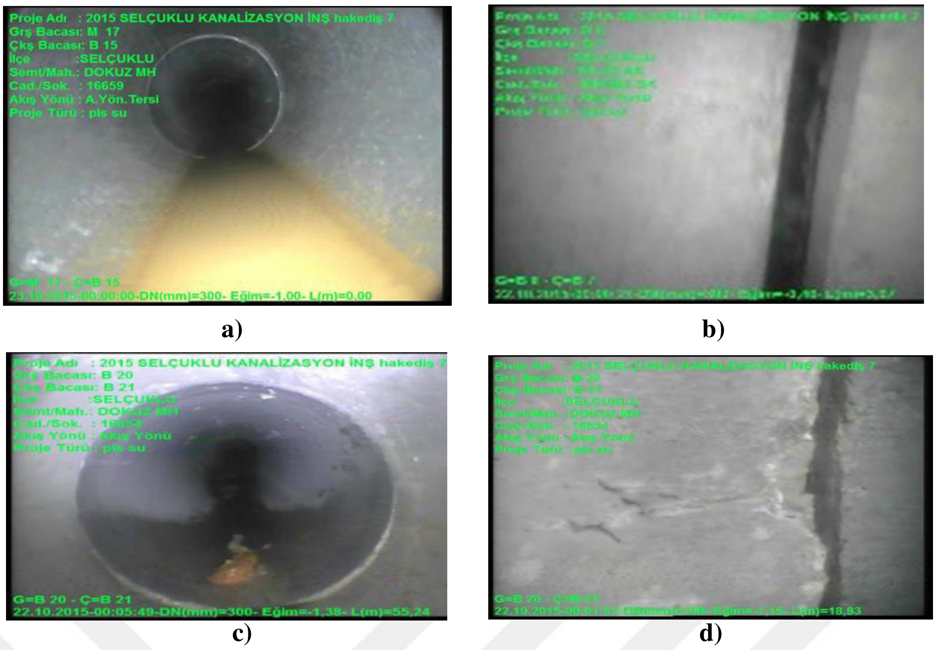

Figure 3.3. images (a) Impurity defect, (b) Additional aperture defect, (c) Residues defect and (d) Capillary fraction defect, given by the robot from inside

Figure (3.3. (a, b, c, and d)) shown defects that may occur in the non-metal sewer underground pipelines. These disorders may be discovered by extracting the characteristic from interior image taken from inside the pipes as a videos. These videos have been taken from the company mentioned previously, submitted to predesigned program to convert them into frames (one frame each one second). The frames were categorized into 4 classes (dataset); Impurities (36 images), Additional aperture (33 images), Residues (27 images) and Capillary fraction (23 images). Datasets were classified into classes and used as inputs to detect these defects through extracting their characteristics.

3.2. Methods

3.2.1. Filters

To enhance the images that extracted and classified from the videos, different filters were used. These images passed into filters to eradicate noises that may occur during the process of filming of the video and make them more clearly.

3.2.1.1. Sobel Operator (SO)

In general SO is used in edge detection algorithms to produce image through concentrating on edge and transitions of the image. Irwin Sobel was the inventor of this operator (Sobel, 2014) and named after this inventor. This operator contain two convolution 3*3 matrices (kernels). The first is for estimation gradient X-axis (row) and the second estimates Y-axis slop, which are columns (Othman et al., 2009). This algorithm based on first derivative convolution, analyses derivatives and estimation the gradient of the image intensity at each point, and then it gives the direction to boost the image intensity at each point from light to dark. It plots the edges at the points where the gradient is highest (Poobathy and Chezian, 2014).

$$G_x = \begin{pmatrix} -1 & 0 & +1 \\ -2 & 0 & +2 \\ -1 & 0 & +1 \end{pmatrix} \quad G_y = \begin{pmatrix} +1 & +2 & +1 \\ 0 & 0 & 0 \\ -1 & -2 & -1 \end{pmatrix}$$

Figure 3.4. Sobel convolution Mask

Figure (3.4.) reflects two matrices G_x and G_y, where G is gradient, x and y represent horizontal and vertical mask axis respectively. These G_x and G_y are integrated to find the gradient at evry point (Poobathy and Chezian, 2014). Then the absolute gradient bulk will be given by equatiıon (3.1):

$$|G| = \sqrt{G_x^2 + G_y^2} \tag{3.1}$$

But often this value is approximated with (Maini and Aggarwal, 2009):

$$|G| = |G_x| + |G_y| \tag{3.2}$$

This operator can smooth the impact of disordered noises in an image. It is differentially isolated by two rows and columns, so the edge parts on both sides become enhanced. This may give bright and thick look of the edges (Maini and Aggarwal, 2009). Figure (3.5.) shows image obtained after applying Sobel filter.

Figure 3.5. (a) Original image (b) Image Obtained After Applying Sobel Filter

3.2.1.2. Prewitt operator (PO)

It is resembling to Sobel, gradient based operator which compute first derivative. Here $3 * 3$ masks are utilized to find out the peak gradient magnitude. When the highest magnitude found, then it works on that direction. Boundaries are detected by the way of either horizontal or vertical manner or both. The figure (3.6.) reflects the 3 x 3 kernels of PO, it uses first derivative to find gradient (Poobathy and Chezian, 2014).

$$G_x = \begin{pmatrix} -1 & -1 & -1 \\ 0 & 0 & 0 \\ 1 & 1 & 1 \end{pmatrix} \quad G_y = \begin{pmatrix} -1 & 0 & 1 \\ -1 & 0 & 1 \\ -1 & 0 & 1 \end{pmatrix}$$

Figure 3.6. Prewitt convolution mask

3.2.1.3. Robert's cross operator

The simple approximation to gradient magnitude based operator provides $2 * 2$ neighborhood of the current pixel. Its convolution masks are,

$$G_x = \begin{pmatrix} 1 & 0 \\ 0 & -1 \end{pmatrix} \qquad G_y = \begin{pmatrix} 0 & 1 \\ -1 & 0 \end{pmatrix}$$

Figure 3.7. Robert's convolution mask

The figure (3.7.) shows two matrices G_x and G_y, where G is gradient, x and y are horizontal and vertical mask axis (Poobathy and Chezian, 2014).

3.2.1.4. Canny Operator (CO)

The outstanding algorithm utilizes four major processes to reach virtual edge of a digital image. The four processes are; smoothing, derivation, maxima finding, and thresholding. The first one gives smooth image for conducting the second goal (i.e. derivative of Gaussian); third step is to achieve maxima after derivation. Final process of CO is hysteresis thresholding. The achievement of this Gaussian-based operator is done because of its low error rate and well localization of edge points. Besides, it provides solo boundary. To fulfill this, smoothing is done. Two level thresholding are followed in this way, the weak boundaries are included in the edge map only if it is connected with strong boundary lines (Poobathy and Chezian, 2014).

3.2.1.5. Median Filter (MF)

MF is a non-linear method, used to eradicate noise from images (Mustafa et al., 2012). E.g., salt and pepper noise can be easily minimized by MF. The MF can eradicate noise actively while preserving edges, this is one of its most important features. This is why MF is often used in image segmentation task as we know the importance of the rule played by edges in the process. The procedure of this filter is: it moves through the image pixel by pixel exchanging each value by median value of the nearby pixels (Mittal and Anand, 2013; Bora and Gupta, 2014). The pattern of the neighbors is called the window, which slides, pixel by pixel, over the whole image. The MF is then compute by first sorting all the pixel values from the window into numerical order. Finally, exchange the considering pixel with the median pixel value (Bora et al., 2015).

3.2.2. Algorithms

3.2.2.1. The k-means clustering

The data clustering techniques are important methods to be used by workers dealing with huge databases having data of many variables. On the other hand, it is a method for analyzing data of descriptive nature in order to reveal composition found in the data (Morissette and Chartier, 2013). Data clustering technique is very easy and applicable method for partition datasets, it aims to yield groups of cases or variables having high level of resemblance in the single group as well as minimum level of resemblance among groups (Hastie et al., 2002).

The major concept of this method is to select center points for each group, the number of each is (K). Center is repeatedly selected in random manner. Each point on the dataset is allocated to its nearest center. This could be repeatedly done until there no longer change in the center points of each group, is exist (Dugad and Desai, 1996; Bilmes, 2006). By this way ideal center points can be produced.

Most of previous research's choose 3 K-means clustering algorithms: - The Forgy/Lloyd algorithm, the MacQueen algorithm and the Hartigan & Wong algorithm. These methods are commonly applied because these techniques almost having slightly different goals and also results. For using any of the above algorithms, in the beginning the number of clusters in the data must be known. This need many tests to find the beast amount of clusters, and data should be standardized as an initiation step in case that ingredients of the cases are not at the same scale. It is well known that there is no absolute best algorithm. The selection of the beast algorithm based on qualities of the datasets regarding size and number of the variables of the case (Morissette and Chartier, 2013). For beast realization of the datasets, many divergent clustering algorithms should be tried (Jain et al., 2000).

3.2.2.1.1. Characteristics of some clustering algorithms:

- Lloyd: it is important in its use for sets of huge data, data distribution is distinguished and the optimization of total sum squares. On the other hand, its disadvantages are slowly in the converge process and some empty clusters may be created (Morissette and Chartier, 2013).
- Forgy: This algorithm possesses same advantages in Lloyd algorithm except for the data distribution which is here is continuous. As for the disadvantages, they are resembled with that of Lloyd method (Morissette and Chartier, 2013).
- MacQueen: Initial converge is fast and total sum squares are optimized. Week points in this method are the need to store the two closest-cluster computations for each case, as well as the sensitivity to the system of application of the algorithm to each case (Morissette and Chartier, 2013).

- Hartigan: It is fast in initial converge and make the sum of squares within the cluster optimum. This method however having the same weak points of the MacQueen one (Morissette and Chartier, 2013).

3.2.2.1.2. Clustering algorithm

To find out k cluster the main steps of k-means algorithm are (Steinbach et al., 2000): -

- Choose k points as primary central points.
- Allocate all points to the nearest central point.
- Re-estimate the central point for each cluster.
- Apply steps 2 and 3 repeatedly till the stabilization of the central points.

An algorithm for partitioning (or clustering) N data points into K disjoint subsets S_j containing N_j data points so as to minimize the sum-of-squares criterion equation (3.3).

$$J = \sum_{j-1}^{k} \sum_{n \epsilon s_j} \left| x_n - \varphi_j \right|^2 \qquad (3.3)$$

3.2.2.1.3. Distance metrics

In order to measure the similarity or regularity between the data-items, distance metrics plays a very important role. It is necessary to identify, in what manner the data are interrelated, how various data dissimilar or similar with each other and what measures are considered for their comparison (Singh et al., 2013).

3.2.2.1.3.1. SqEuclidean distance

SqEuclidean distance computes the root of square difference between co-ordinates of pair of objects. The (Euclidean) distance between is found to be Procedure of K-means by equation (3.4) (Singh et al., 2013).

$$d = \sqrt{\sum_{j-1}^{p} (v_{1i} - v_{2i})^2} \qquad (3.4)$$

3.2.2.1.3.2. Cityblock distance

Cityblock estimates the distance between a and b for k times. k is the frequency of estimation. The cityblock distance two point a and b with k dimensions is defined in equation (3.5) (Bora et al., 2014):

$$\sum_{j=1}^{k}\left|a_j - b_j\right| \tag{3.5}$$

3.2.2.1.3.3. Cosine Distance:

The cosine distance between two points is one minus the cosine of the included angle between points (treated as vectors). Given an m-by-n data matrix X, which is treated as m (1-by-n) row vectors x_1, x_2, ..., xm, the cosine distances between the vector $x_s$and x_t are defined as follows equation (3.6) (Bora et al., 2014):

$$d_{st} = 1 - \frac{x_s x_t^{-}}{\sqrt{(x_s x_s^{-})(x_t x_t^{-})}} \tag{3.6}$$

3.2.2.2. Feature Extraction (FE)

A substantial realm of Artificial intelligence in (FE). It is extraction of the more suitable and interested features of an image and assign it into label. The substantial step in image categorization is the analysis of the image qualities and arrange these results the numerical features into categories. The mean the image categorized on the basis of its content (Morales-González et al., 2014; Seyyedi and Ivanov, 2014).

Categorization model and accuracy rate is depending upon the numerical qualities of different image features that represent the data of the categorization model. Recently many feature extraction technique (FET) were mode up each with its own strong and weak points. A suitable FET is the one which gives relevant features (Qian et al., 2013; Xiao et al., 2013).

3.2.2.2.1. Edge detection (ED)

In order to focus on the edge of an image, it is applicable that few weights of the filter be negative. A first-derivative row filter, at a location in the output image, produces variations in pixel values of the columns on both sides of this site of the input image. So, filters output would be grater (either negative or positive) when there are outstanding variations in the values of pixel in the right and left sides of the pixel site. A set of weights, which includes some smoothing in averaging over 3 rows is shown by (Moreno et al., 2009; Fu, 2014):

$$w = \frac{1}{6}\begin{pmatrix} -1 & 0 & 1 \\ -1 & 0 & 1 \\ -1 & 0 & 1 \end{pmatrix}$$

On the contrary second-derivative filters, may be similar and hence, respond to the edges in many orientations, if they remain linear. The arrangement is as follow:

$$w = \frac{1}{3}\begin{pmatrix} 1 & 1 & 1 \\ 1 & -8 & 1 \\ 1 & 1 & 1 \end{pmatrix}$$

It is same kind of filter that is used to make figure (3.8. (c)), i.e. differences among the output from moving average filter as well as the raw image. With these weights, it can be shown that Laplacian transition of $f$equation (3.7) (Fu, 2014).

$$\sum_{k=-1}^{1} \sum_{l=-1}^{1} w_{kl}\, f_{i+k.j+l} \approx \frac{a^2 f_{ij}}{ax^2} + \frac{a^2 f_{ij}}{ay^2} \tag{3.7}$$

Result of using of such filter to $x - ray$ image is gives figure (3.8. (a)). Edges manifest the image as zero-crossing in Laplacian that means the Laplacian will be +ve on one side and –ve in the other one. This is because an edge gives max. and min. values in the first derivative and zero value in the second derivative. Figure (3.8. (b)) gives a tool to identify a zero-crossing, and the –ve and +ve values from the first filter shown as black and white respectively. Hence, zero-crossing match to black/white edges. For reducing the impact of the noise to the minimum level, the filter mentioned above or simple version of Laplacian filter is (Fu, 2014):

$$w = \begin{pmatrix} 0 & 1 & 0 \\ 1 & -4 & 1 \\ 0 & 1 & 0 \end{pmatrix}$$

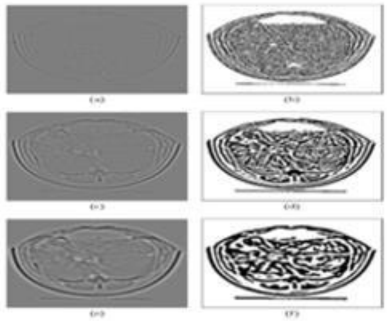

Figure 3.8. second-derivation filters applied to $x - ray$ image (a) 3*3 Laplacian filter, (b) zero-thresholded version of (a), (c) Laplacian-of-Gaussian filter,σ^2=2, (d) zero-thresholded version of (c), (e) Laplacian of Gaussian filter, σ^2=2/3 , (f) zero-thresholded version of (e)

There are three stages of edge detection, pre-processing, feature extraction FE and post-processing. ED process follow is shown figure (3.9.). After pre-processing, of image *I*, a middle result *I* is resulted. This stage emphasizes on noise minimizing and matrix inhibition, while keeping edges as well as the absence of blurring edges between the divergent fields. The feature extraction has two stages: response computation and feature manipulation. In the first stage, estimation can come from statistical data, and a bunch of features R is obtained (Fu, 2014).

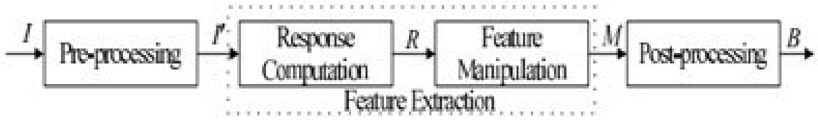

Figure 3.9. General edge detection flow

Feature manipulation stage includes, the choose and buildup of feature, so, the result is a bunch of features M. The FE stage is the main and necessary stage in edge detection. The aim of FE is to apply them to classify pixels as edge points or non-edge points. After post-processing, a final edge map B is resulted. Post-processing mainly emphasizes many manipulating processes, marking edge points, thinning edges, removing stand-alone edge points and linking broken edge points. Generally, a normal pre-processing technique, such as Gaussian filtering, or a popular post-processing technique, such as thinning operations, can in general cooperate with various FET. This survey mainly covers the stage of extracting features. Most commonly used edge detection algorithms are Sobel, Canny, Prewitt, Roberts, zero-cross & Laplacian of Gaussian (Fu, 2014).

3.2.2.3. Color Features (CF)

Color is the main crucial factor for sorting and recovery of the image, and its curve reflects the (CF) procedure. CF, then, is the allocation of color among the image. Image size, rotation and zoom do not affect the CF, and therefore, here its efficiency lies. (Swain and Ballard, 1991; ping Tian, 2013).

3.2.2.3.1. HSV Color Space

HSV Color area HSL or HSI is uni-color field, HSI (or HSV) means hue (H), saturation (S) and intensity (I) (or value V). Review mentions hue as a color character of light. It could be the character of the surface reflecting or transmitting the light. For insistence, a blue sky gives blue hue. In addition, it is a trait of the human feeling (Acharya and Ray, 2005). Figure (3.10.) shown HSV color space.

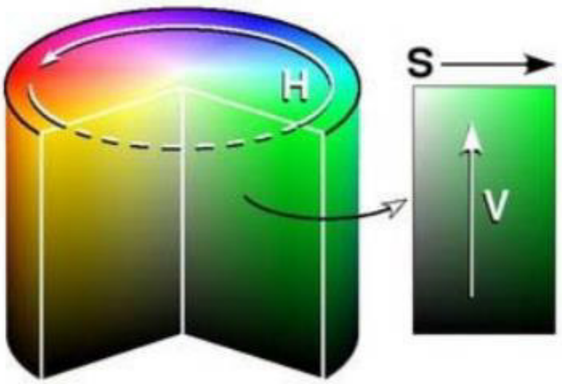

Figure 3.10. HSV color wheel

3.2.2.4. Image Segmentation

In image analysis, segmentation is the partitioning of a digital image into multiple regions (sets of pixels), accorded to some homogeneity criterion (Saraf, 2006). The aim of segmentation is to simplify and/or replace the representation of an image into something that is more significate and easier to analyze (Jameel and Manza, 2012).

There are four approach for image segmentation (Saraf, 2006).

- Threshold techniques.
- Edge based methods (Border of object).
- Region-based techniques.
- Connectivity-preserving relaxation methods.

3.3. Testing of algorithms for defects

To select better algorithm for detecting the defects in our study, each algorithm was applied on 4 defects. The results show that using K-means clustering technique was good enough for detecting of images with Impurities, whereas, for Additional aperture defect, edge detection technique is being the best to identify this type of defects. For image having objects as Residues, color feature (HSV color space) was the best method. Finely as for the Capillary fractions, image segmentation technique gave the best results.

3.3.1. Testing of K-means clustering algorithm

Distance measure

That K-means clustering should minimize with respect to type of distance measure for instance:

- SqEuclidean: Square Euclidean distance.
- Cityblock: Some of absolute differences.
- Cosine: One minus the cosine of the included angle between points.

Start

Method use to choose initial cluster centroid position such us:

- Sample: Select K observation from X at random.
- Uniform: Select K point uniformly at random from range of X.
- Matrix: Matrix of starting location.

The distance between the element and the center of the cluster plays an important role in clustering process. Through picking up the suitable measuring mean, better and more accurate results in diagnosing the defect, would be gained. The method of selection starting point of the cluster, is also an important factor in carrying out clustering process. Therefore, K-means clustering technique was examined by selection of many types for distance measuring methods, as well as, many methods of starting center of the cluster. The algorithm was applied on dataset having some defects (i.e. Impurity, Additional aperture, Residues and Capillary fraction). Results are arraigned in the tables (3.1.), (3.2.), (3.3.) and (3.4.) respectively:

Table 3.1. Effect of start point and distance measuring method on accuracy of Impurity detect algorithm using dataset have **Impurity** defects (%)

Distance Measurment Method \ Madde	Sample	Uniform	Matrix
SqEuclidean	53.1	56.3	**100**
Cityblock	15.6	31.3	96.9
Cosine	25	25	87.5

Table 3.2. Effect of start point and distance measuring method on accuracy of Impurity detect algorithm using dataset have **Additional aperture** defects (%)

Distance Measurment Method \ Madde	Sample	Uniform	Matrix
SqEuclidean	8.3	91.7	16.7
Cityblock	16.7	50	8.3
Cosine	8.3	50	25

Table 3.3. Effect of start point and distance measuring method on accuracy of Impurity detect algorithm using dataset have **Residues** defects (%)

Distance Measurment Method \ Madde	Sample	Uniform	Matrix
SqEuclidean	92.8	92.8	92.8
Cityblock	85.7	92.8	92.8
Cosine	92.8	92.8	92.8

Table 3.4. Effect of start point and distance measuring method on accuracy of Impurity detect algorithm using dataset have **Capillary fraction** defects (%)

Distance Measurment Method \ Madde	Sample	Uniform	Matrix
SqEuclidean	0	60	0
Cityblock	0	40	0
Cosine	20	60	0

It is obvious from the data in the above tables that this algorithm is very applicable for prescribe and identification for any Impurity may present in the pipes.

3.3.2. Testing of edge detection algorithm

To find out the additional aperture algorithm performance and defect diagnosing accuracy, a group of edge detection operator was examined with a group of median filter size. The algorithm was applied on dataset having some defects (i.e. impurity, additional aperture, residues and capillary fraction). Results are arraigned in the tables (3.5.), (3.6.), (3.7.) and (3.8.) respectively:

Table 3.5. Effect of edge detection operator and median mask size on accuracy of Additional aperture detect algorithm using dataset have **Impurity** defects (%)

Median Mask Size / Edge operator	[3 3]	[5 5]	[7 7]	[9 9]	[11 11]	[13 13]
Sobel	3.13	6.25	3.13	3.13	3.13	3.13
Canny	0	3.13	3.13	3.13	3.13	3.13
Prewitt	3.13	6.25	3.13	3.13	3.13	3.13
Roberts	0	0	0	0	0	0

Table 3.6. Effect of edge detection operator and median mask size on accuracy of Additional aperture detect algorithm using dataset have **Additional aperture** defects (%)

Median Mask Size / Edge operator	[3 3]	[5 5]	[7 7]	[9 9]	[11 11]	[13 13]
Sobel	91.6	**100**	**100**	91.6	91.6	91.6
Canny	33.6	33.6	33.6	33.6	33.6	33.6
Prewitt	**100**	**100**	**100**	91.6	**100**	**100**
Roberts	91.6	83.3	83.3	83.3	**100**	83.3

Table 3.7. Effect of edge detection operator and median mask size on accuracy of Additional aperture detect algorithm using dataset have **Residues** defects (%)

Median Mask Size / Edge operator	[3 3]	[5 5]	[7 7]	[9 9]	[11 11]	[13 13]
Sobel	14.29	7.14	14.29	14.29	14.29	7.14
Canny	0	0	14.29	14.29	7.14	14.29
Prewitt	14.29	7.14	14.29	14.29	14.29	7.14
Roberts	7.14	7.14	14.29	7.14	14.29	7.14

Table 3.8. Effect of edge detection operator and median mask size on accuracy of Additional aperture detect algorithm using dataset have **Capillary fraction** defects (%)

Median Mask Size / Edge operator	[3 3]	[5 5]	[7 7]	[9 9]	[11 11]	[13 13]
Sobel	60	60	20	20	20	40
Canny	60	60	60	60	60	60
Prewitt	60	60	20	20	20	40
Roberts	40	20	20	40	60	20

It is obvious from the data in the above tables that this algorithm is very applicable for prescribe and identification for any Additional aperture may present in the pipes.

Below tables explain the time required for application of additional aperture. Data in table (3.6.) reflects that 100 % accuracy cases appeared serval times. Therefore, time element was applied to accomplish ideal solution in discovery of additional aperture from the accuracy and time points of view. Table (3.9.) below show the time taken to apply the algorithm:

Table 3.9. Execution time for applying Additional aperture detect algorithm (seconds)

Median Mask Size / Edge operator	[3 3]	[5 5]	[7 7]	[11 11]	[13 13]
Sobel	-	**2.34**	2.43	-	-
Prewitt	2.36	2.36	2.40	2.38	2.49
Roberts	-	-	-	2.35	-

3.3.3. Testing of color space algorithm

In applying residues defect discovery, two main factors were manipulated to gain accurate results in defect identification. These factors were saturation elevation and threshold to isolate the high saturation degrees from the processed image. The algorithm was applied on dataset having some defects (i.e. impurity, additional aperture, residues and capillary fraction). Results are arraigned in the tables (3.10.), (3.11.), (3.12.) and (3.13.) respectively:

Table 3.10. Effect of different values of saturation and threshold of segment binary mask on accuracy of Residues detect algorithm using dataset have **Impurity** defects (%)

Value of saturation / Threshold Binary Mask	1.0	1.1	1.2	1.3	1.4	1.5	1.6	1.7	1.8	1.9	2.0
0.1	9.38	9.38	6.25	3.13	3.13	3.13	3.13	3.13	3.13	3.13	3.13
0.2	28.1	28.1	28.88	15.63	12.2	12.5	12.5	12.5	12.5	9.38	9.38
0.3	18.7	6.25	31.95	28.13	28.13	34.38	18.75	25	21.88	18.75	15.63
0.4	12.5	6.25	12.5	18.75	24.24	18.75	31.25	28.1	25	25	28.13
0.5	0	3.13	12.5	9.38	6.25	12.5	25	18.7	28.13	28.13	28.13
0.6	0	0	0	0	6.25	0	0	12.5	18.75	25	18.75
0.7	0	0	0	0	0	0	0	0	0	9.38	12.5
0.8	0	0	0	0	0	0	0	0	0	12.5	12.5

Table 3.11. Effect of different values of saturation and threshold of segment binary mask on accuracy of Residues detect algorithm using dataset have **Additional aperture** defects (%)

Value of saturation / Threshold Binary Mask	1.0	1.1	1.2	1.3	1.4	1.5	1.6	1.7	1.8	1.9	2.0
0.1	8.3	16.7	25	25	25	16.7	16.7	16.7	16.7	8.3	16.7
0.2	8.3	0	0	8.3	16.7	16.7	8.3	8.3	8.3	8.3	8.3
0.3	0	0	0	0	0	8.3	0	0	0	0	0
0.4	0	0	0	0	0	0	0	0	0	0	0
0.5	0	0	0	0	0	0	0	0	0	0	0
0.6	0	0	0	0	0	0	0	0	0	0	0
0.7	0	0	0	0	0	0	0	0	0	0	0
0.8	0	0	0	0	0	0	0	0	0	0	0

Table 3.12. Effect of different values of saturation and threshold of segment binary mask on accuracy of Residues detect algorithm using dataset have **Residues** defects (%)

Value of saturation / Threshold Binary Mask	1.0	1.1	1.2	1.3	1.4	1.5	1.6	1.7	1.8	1.9	2.0
0.1	14.3	92.8	7.1	7.1	7.1	0	0	0	0	0	0
0.2	50	50	42.9	35.7	35.7	35.7	28.6	28.6	28.6	28.6	14.3
0.3	87.6	**100**	85.7	57.1	57.1	50	50	42.9	42.9	35.7	35.7
0.4	57.1	57.4	57.1	78.6	78.6	**100**	85.7	64.3	57.1	57.1	50
0.5	14.3	28.5	50	35.7	42.9	57.1	57.1	92.9	92.9	92.9	85.7
0.6	0	7.1	14.3	28.6	42.9	57.1	50	50	57.1	57.1	78.6
0.7	0	0	0	7.1	14.3	14.3	28.6	50	57.1	57.1	50
0.8	0	0	0	0	0	0	14.3	21.4	35.7	42.9	57.1

Table 3.13. Effect of different values of saturation and threshold of segment binary mask on accuracy of Residues detect algorithm using dataset have **Capillary fraction** defects (%)

Threshold Binary Mask \ Value of saturation	1.0	1.1	1.2	1.3	1.4	1.5	1.6	1.7	1.8	1.9	2.0
0.1	0	0	0	20	40	40	40	40	40	40	60
0.2	0	0	0	20	20	0	0	0	0	0	0
0.3	0	0	0	0	0	0	0	0	0	0	0
0.4	0	0	0	0	0	0	0	0	0	0	0
0.5	0	0	0	0	0	0	0	0	0	0	0
0.6	0	0	0	0	0	0	0	0	0	0	0
0.7	0	0	0	0	0	0	0	0	0	0	0
0.8	0	0	0	0	0	0	0	0	0	0	0

It is obvious from the data in the above tables that this algorithm is very applicable for prescribe and identification for any Residues may present in the pipes.

Below tables explain the time required for application of Residues algorithm. Data in table (3.12.) also reflects that 100 % accuracy cases appeared more than one time. So, it was successful to exploit the time element once again to achieve the proper solutions to discover the residues as accurate and swift as possible. Below the time required for application of this algorithm presented in table (3.14.):

Table 3.14. Execution time for applying Residues detect algorithm (seconds)

Threshold Binary mask \ Value of saturation	1.1	1.5
0.3	**4.44**	-
0.4	-	4.48

3.3.4. Testing of image segmentation algorithm

An important two factors with applying capillary fraction identification algorithm, are obviously impact the efficiency and accuracy of the used algorithm. The first is the operator type used in edge detection technique, whereas, the second is, also, the threshold factor. In this realm, divergent types of operators, and many levels of threshold factor were selected to carry out this study. The algorithm was applied on dataset having some defects (i.e. impurity, additional aperture, residues and capillary fraction). Results are arraigned in the tables (3.15.), (3.16.), (3.17.) and (3.18.) respectively:

Table 3.15. Effect of edge operator and threshold factor on accuracy of Capillary fraction detect algorithm using dataset have **Impurity** defect (%)

Threshold factor / Edge operator	0.1	0.2	0.3	0.4	0.5	0.6	0.7	0.8	0.9	1.0	1.1	1.2
Sobel	0	0	0	0	0	3.13	6.25	12.50	6.25	6.25	0	0
Canny	0	0	0	0	0	0	0	0	0	0	0	0
Prewitt	0	0	0	0	0	3.13	0	6.25	12.50	0	0	0
Roberts	0	0	0	0	0	3.13	0	9.37	9.37	3.13	0	0

Table 3.16. Effect of edge operator and threshold factor on accuracy of Capillary fraction detect algorithm using dataset have **Additional aperture** defect (%)

Threshold factor / Edge operator	0.1	0.2	0.3	0.4	0.5	0.6	0.7	0.8	0.9	1.0	1.1	1.2
Sobel	0	0	8.3	8.3	16.7	33.3	8.3	0	16.6	25	25	8.3
Canny	0	0	0	0	0	0	0	0	0	0	0	0
Prewitt	0	0	8.3	8.3	33.3	16.6	8.3	16.6	8.3	25	25	0
Roberts	0	0	8.3	25	25	16.6	16.6	0	0	16.6	25	25

Table 3.17. Effect of edge operator and threshold factor on accuracy of Capillary fraction detect algorithm using dataset have **Residues** defect (%)

Threshold factor / Edge operator	0.1	0.2	0.3	0.4	0.5	0.6	0.7	0.8	0.9	1.0	1.1	1.2
Sobel	0	0	0	0	0	0	0	0	0	0	0	0
Canny	0	0	0	0	0	0	0	0	0	0	0	0
Prewitt	0	0	0	0	0	0	0	0	0	0	0	0
Roberts	0	0	0	0	0	0	0	0	0	0	0	0

Table 3.18. Effect of edge operator and threshold factor on accuracy of Capillary fraction detect algorithm using dataset have **Capillary fraction** defect (%)

Threshold factor / Edge operator	0.1	0.2	0.3	0.4	0.5	0.6	0.7	0.8	0.9	1.0	1.1	1.2
Sobel	0	0	20	0	40	60	40	60	**100**	40	0	0
Canny	0	0	0	0	0	0	0	0	0	0	0	0
Prewitt	0	0	0	0	40	60	40	60	60	40	0	0
Roberts	0	0	0	0	40	40	40	40	60	60	40	0

It is obvious from the data in the above tables that this algorithm is very applicable for prescribe and identification for any Capillary fraction may present in the pipes.

3.4. Implementation of algorithms

3.4.1. Implementation of K-means clustering algorithm

The locations of the impurities in the images contained them, are slightly differ in color from the other parts of the image. This is an important character for the image including this type of defects. This trait was used in this investigation to detect impurities present in the input images as shown in figure (3.11.), by employing K-means clustering technique.

Figure 3.11. Image contained impurity

This technique is the most common algorithm used in data analysis due to its simplicity and distinguished mathematical performance, based it can be applied to evaluate datasets on the bases of clustering them into 2-clusters, one of them contains similar characteristics represent the impurities that are the important part to be gained, regardless the other data of the image. That is why the selection was classified them into cluster (i.e. no. of clusters = 2). Similitude scale (Euclidian distance) was employed in this study. This scale, however, plays an important role in classification and finding out datasets, depending upon the similitude of these data and ultimately finding the center point for each group.

The classification output was index 1 and 2, where (1) represent the first cluster, whereas (2) is the second one as shown in figure (3.12.).

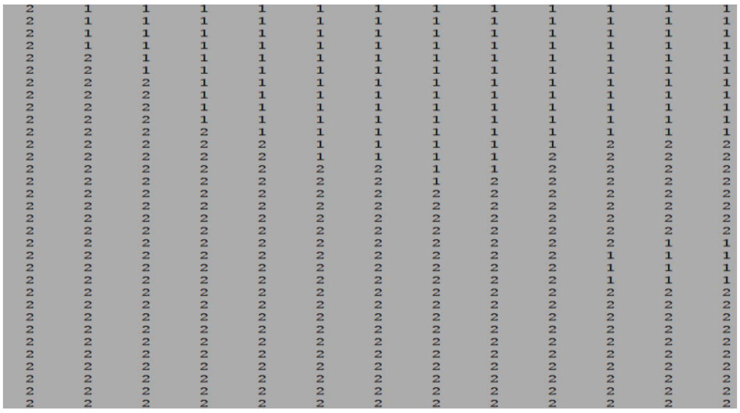

Figure 3.12. Output image indexed by 0 and 1

The index was converted into image, in this image the pixels with 255 value is the impurities, and pixels with 0 value is the other data in the original image, figure (3.13.) illustrate the output image.

Figure 3.13. Image results by converting index

Finally, in this trial it was found that the object was the impurities, and by estimates and study its characters (area, length, and width) as measurement units, it was possible to distinguish the image having this type of defects from the other image of datasets.

Image analysis as well as finding the number of objects in the image helped in understanding and manifestation of image contents and finally make a suitable decision whether these images contain impurities. Image with object = 0 is free of impurities and the vice is not always versa. The image with impurities could analysis and the information may be extracted by estimating the area of the object which is sum of pixels within the object that can be used as measurement unit. Here, in the image containing impurities as a defect, the object area would be greater as compared to that free of this defect.

3.4.1.1. Flowchart and the code of Impurity defect

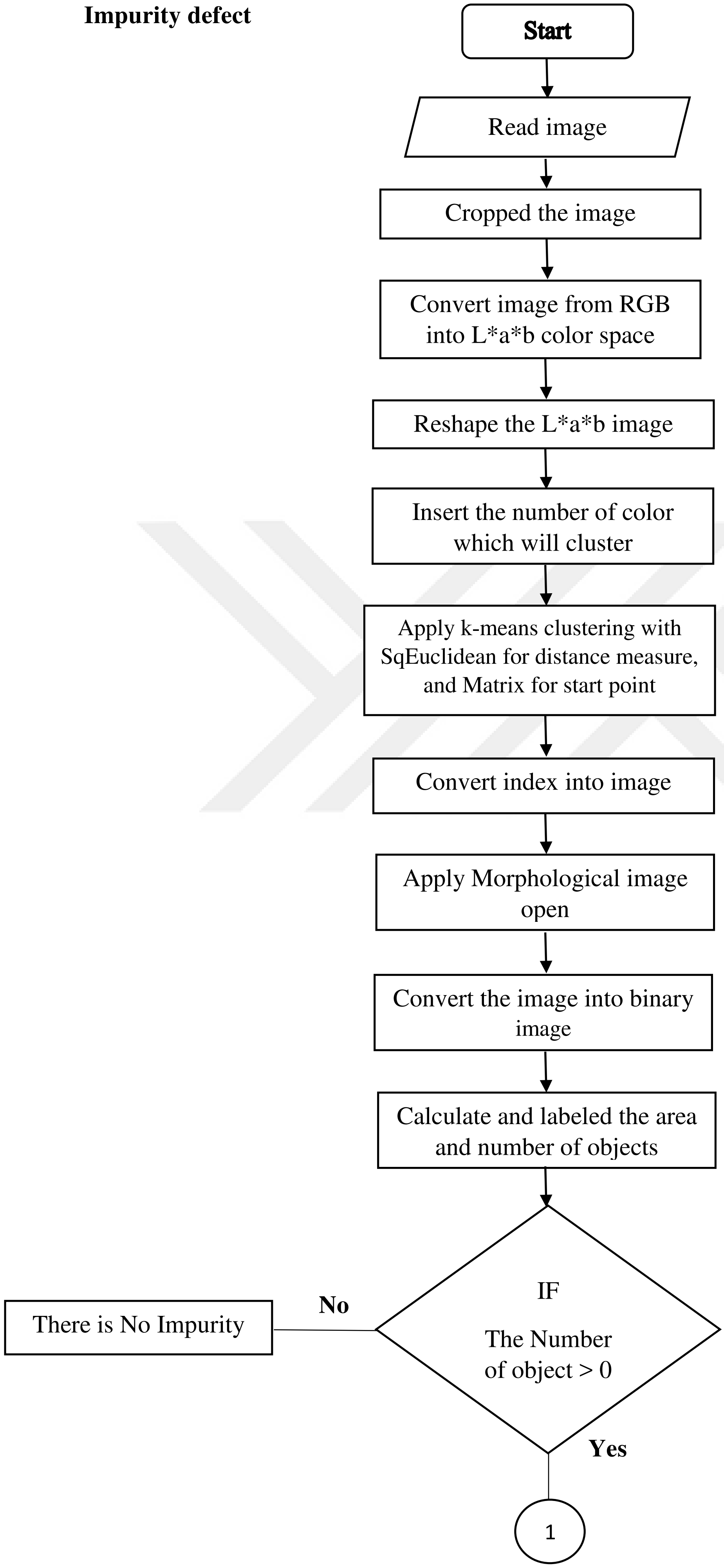

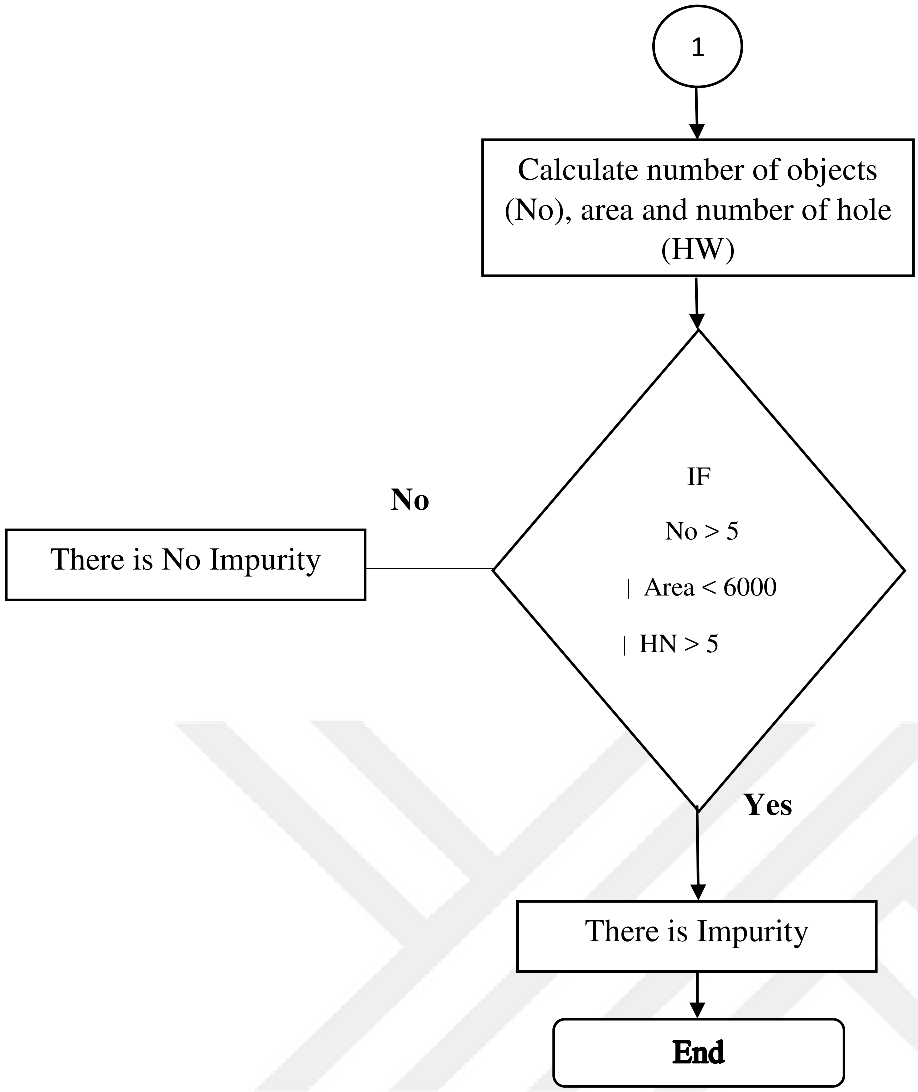

Flowchart 1 Impurity detection algorithm

The code of impurities algorithm

```
function  z  = Mildet( im )
he=im;
rect=[0 40 630 570];
I2 = imcrop(he,rect);
A=I2(1:180,:,:);
B=I2(180+1:end,:,:);
B1=imcrop(B,[11 0 630 300]);
[m n k]=size(B1);
cform = makecform('srgb2lab');
lab_he = applycform(B1,cform);
ab = double(lab_he(:,:,2:3));
nrows = size(ab,1);
```

```
ncols = size(ab,2);
ab = reshape(ab,nrows*ncols,2);
C=[m 55; m 54;m 22];
Seed = [1 1; 270 260];
nColors =2;
[cluster_idx] = kmeans1(ab,nColors,'distance','sqEuclidean',  'Start',Seed);
 pixel_lapels = reshape(cluster_idx,nrows,ncols);
  I=pixel_labels;
[m n] =size(I);

for i=1:m
   for j=1:n

      if I(i, j)==1
         p(i, j)=0;
      else
         p(i, j)=255;
      end
   end
end

se = strel('disk',7);
p = imopen(p,se);
level=graythresh(p);
 bw=im2bw(p,level);
[labeled,numObjects]=bwlabel(bw,4);
info=regionprops(labeled,'all');
 if(numObjects>0)
info(1).Area;
 Areas=cat(1,info.Area);
  mask=logical(p);
red=immultiply(mask,B1(:,:,1));
g=immultiply(mask,B1(:,:,2));
b=immultiply(mask,B1(:,:,3));
```

```
im=cat(3,red,g,b);
[m n k]=size(im);
I=reshape(im,m*n,3);
idx=find(mask);
level=graythresh(p);
bw=im2bw(p,level);
 [labeled,numObjects]=bwlabel(bw,4);
info=regionprops(labeled,'all');
Euler_Number1=info(1).EulerNumber;
NumHoles1=1-Euler_Number1;
bigest_Area=info(1).Area;
l=1;
for i=2:numObjects
 if(bigest_Area<info(i).Area)
    bigest_Area=info(i).Area;
    l=i;
end
end
 in=find(cat(1,info.Area)==bigest_Area);
[m n K]=size(B1);
No=numObjects;

HN=NumHoles1 ;
area=bigest_Area;
if ( area < 7140  )
         disp ('there are No impurities');
       z=0;
else
         disp ('there are impurities');
       z=1;
end
else
      disp ('here no impurities');
    z=0;
```

```
end
end
```

3.4.2 Implementation of edge detection algorithm

Image with additional apertures (aperture of the joint between pipes) are characterized with discontinuity or sudden change in some optical properties such as, light intensity, structure or color. Therefore, for such image with these defects, edge detection technique was applied as shown down in figure (3.14.).

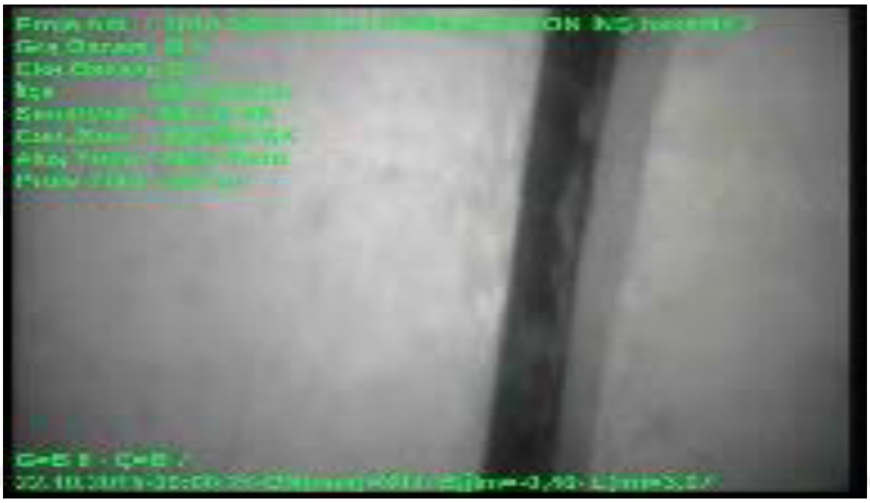

Figure 3.14. Additional aperture image

The basic concept of this technique is that, the edge information could be found through the relationship between each pixel in the image with the surrounding pixels. Edges in this types of image comprise specific useful information for image analysis and detect the additional apertures as well. Sobel operator with threshold equal to 0.020 was followed to detect the image edge. The function of this technique was to lineation of the objects of the image (i.e. additional apertures) by boosting the image brightness, eliminating many un-useful information in image analysis process. After applying the technique, bi-sector image with additional apertures boarders was obtained, in addition to presence of some edges inside and outside the apertures boarders as noise as shown in figure (3.15.) bellow.

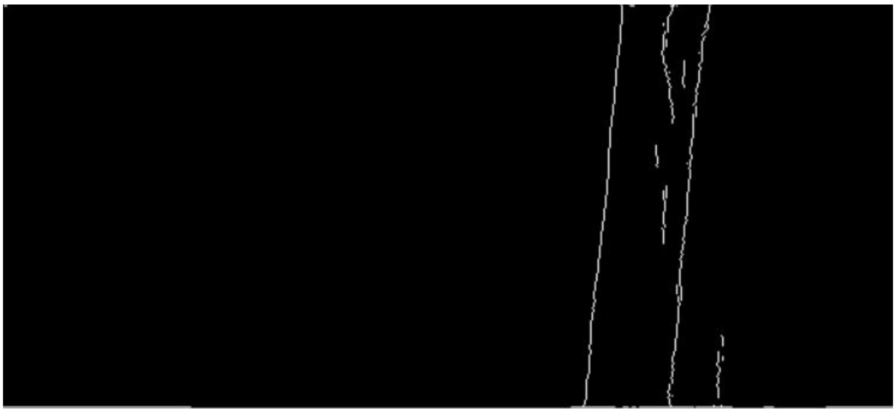

Figure 3.15. Applying Sobel with threshold 0.020

The next step was the elimination of the noise inside and outside the object (apertures). By image close morphological technique, that is dilation followed by erosion. So, the result was logical image of background which is (0) value and additional apertures which have the value (1) for the pixels, figure (3.16.) bellow illustrate the output logical image.

Finally, the properties of the object (apertures) were used as measurement units for measure and comparison to detect the image having additional apertures as defect.

Figure 3.16. The output logical image.

This line was analyzed and its properties were extracted and used for distinguish the image containing such type of defects from the other images. For instance, the length of the object was measured and used to verify whether object additional aperture or not. Length was used for further analysis, if it is less two-thirds of the image length so, this object is not additional aperture. On the other hand, object width has an importance not less than the importance of the length quality. Width has also been measured and used to identify the defect, in the sense that the width of the object does not exceed one third of the original image and not less than 20 pixels. Some time, the output may contain some other extra objects which are noises hindering the discovery process, whereas in this study this noises were exploited to be another feature help in the discovery process, in the sense that the image having defect, its noise does not exceed than (5) objects, otherwise, it is free of additional aperture.

3.4.2.1. Flowchart and the code of Additional aperture defect

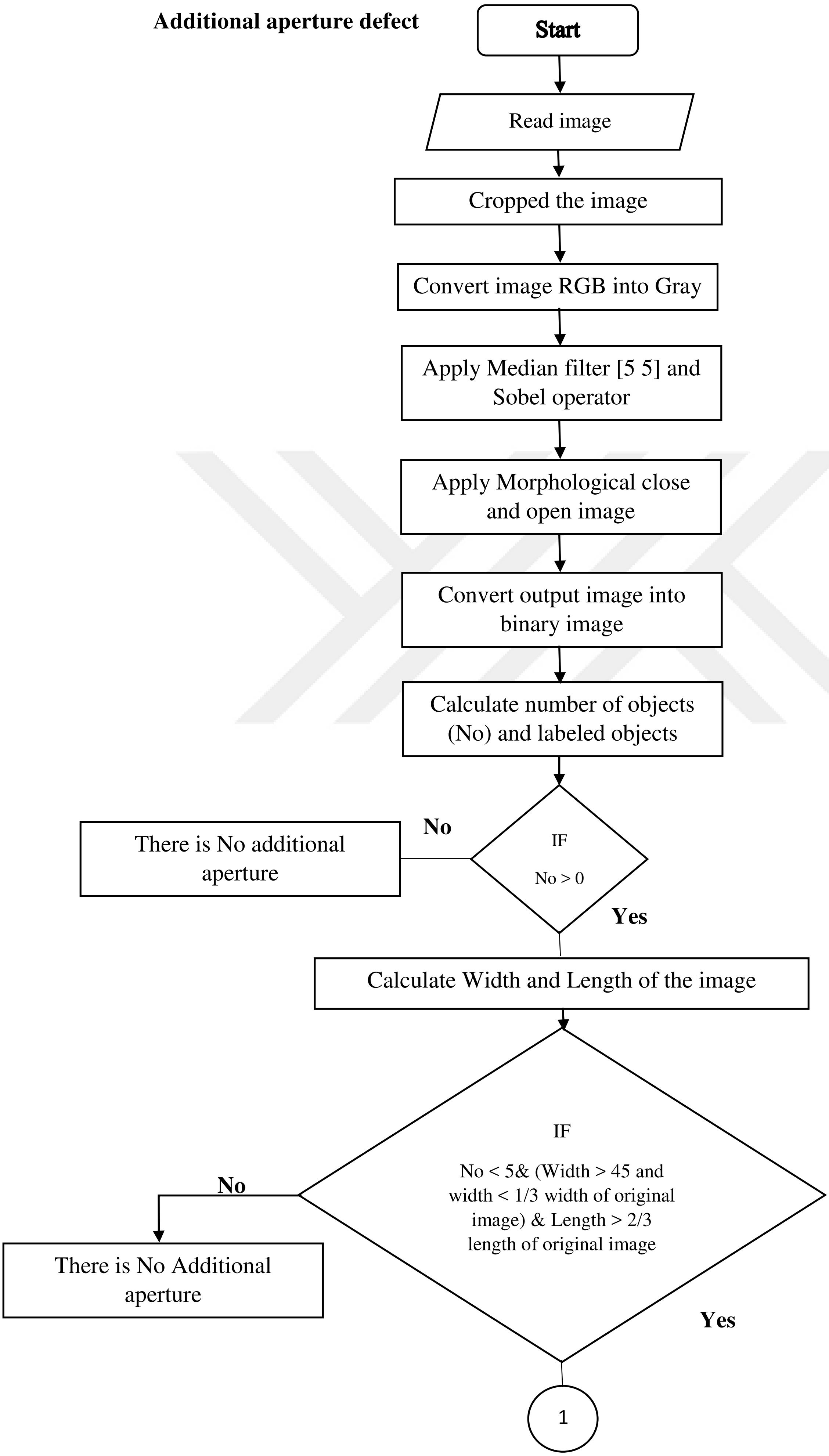

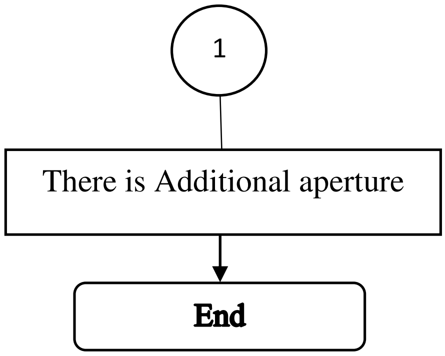

Flowchart 2 Additional aperture detect algorithm

The code of additional aperture

```
function A = AddAperture( im )
rgb=im;
rect=[0 40 630 570];
I2 = imcrob(rgb,rect);
A=I2(1:180,:,:);
B=I2(180+1:end,:,:);
A1=imcrop(A,[250 0 630 180]);
B1=imcrop(B,[11 0 630 250]);
h = ones(2,8)/7.8;
rgb2 = imfilter(B1,h);
b=rgb2gray(rgb2);
b= medfilt2(b, [5 5]);
c2=edge (b,'sobel', 0.020);
se = strel('disk',38);
closeBW = imclose(c2,se);
rect=[28 6 590 230];
I2 = imcrop(closeBW,rect);
I2 = bwareaopen(I2, 200);
I2= double(I2);
level=graythresh(I2);
 bw=im2bw(I2,level);
[labeled,numObjects]=bwlabel(bw,4);
info=regionprops(labeled,'all');
```

```
  level=graythresh(I2); bw=im2bw(I2,level);
 [labeled,numObjects]=bwlabel(bw,4);
info=regionbrops(labeled,'all');
if (numObjects > 0)
Extrema1=info(1).Extrema ;
width=Extrema1(2,1)-Extrema1(1,1);
lenght=Extrema1(6,2)-Extrema1(1,2);
 [m n k]=size(I2);
   if (numObjects <5 && width >20  && width< (n/(2+1)) && lenght> m-30  )
 disp(sprintf('there are additional aperture' ));
A=1;
else
disp(sprintf('there are  NOO aperture'));
A=0;
end
else
disp(sprintf('there are  NO00 aperture'));
A=0;
end
end
```

3.4.3. Implementation color feature extraction algorithm

The most common used in this regard is the colored image partition rather than gray-level because of its high ability to analysis the image and ultimately improve the segmentation results. Employing the colored segmentation and section of the suitable color space, is of high importance because that leads to better results. By applying color image segmentation, it was possible to detect residues within the image. By controlling color space, on the other have, excellent results were gained particularly the object (residues) show a saturation level higher than the rest parts of the image as shown in figure (3.17.). Thus, the image was transformed form RGB color space into HSV color space and the saturation level of the object was augmented as shown below in figure (3.18.), array contain saturation which is the second array in this image was resulted.

Figure 3.17. Residues image

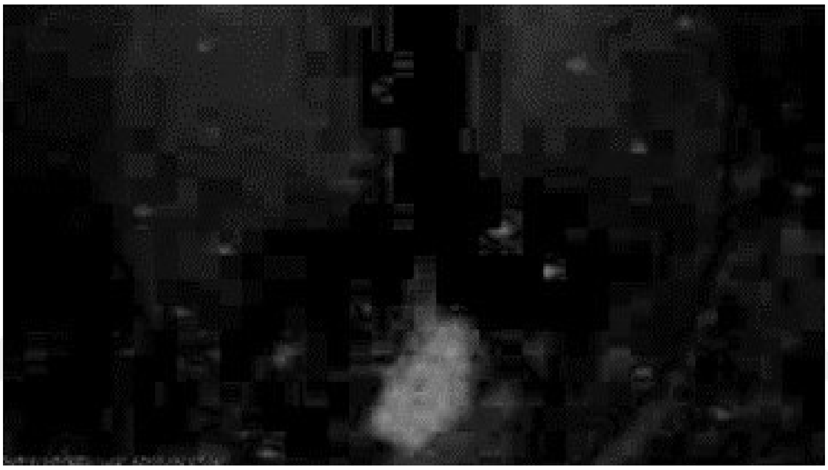

Figure 3.18. Saturation image

After saturation image was yielded, image was divided by convolution of 3*3 mask on the image, the result was image contain only the objects with high level of saturation plus a little noise figure (3.19.) below show the result. Applying Morphological open image then Morphological close image for image analysis, the output was an image contain the residues as groups of objects. The objects were labeled and by measuring the area of each object and the total area of the objects it was possible to identify and detect residues containing image.

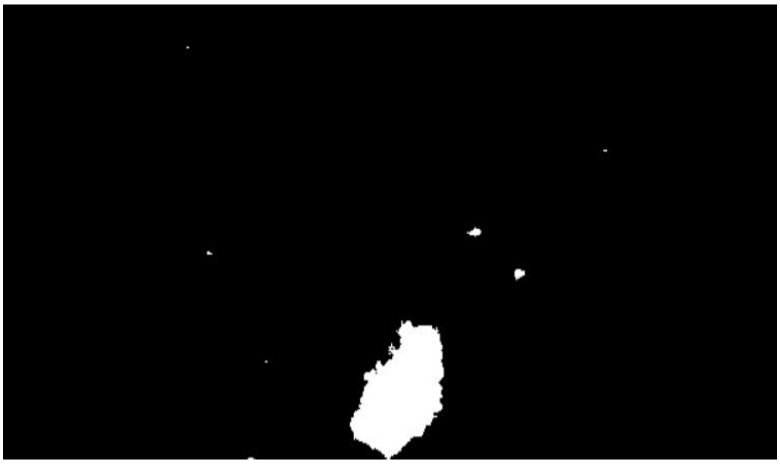

Figure 3.19. Residues with some noise

The output images were analyzed to count the number of the objects in each image, beside, the object area and the nature of the pixels inside the object were also studied. For identification and comparison, the test was finding out the number of objects, if number of objects is more than one, here, the total objects area was estimated and used as comparison element for diagnosing the images having residues. Whereas if the object number is one, the object area has also been estimated and used for comparison process.

More accurate analysis of the output images resulted in finding some white color locations beside the residues. The white color means they are with high pixel's values. They appeared because of their high level saturation. To distinguish between these white spots and the real residues, their pixel's values were used as comparison elements and distinguishing points, bearing in mind that the values of the object (residues) are lower than that of these white spots. Thus, means of the objects were estimated and compared with the threshold. The high value means, always belongs to the white spots, whereas low means belongs to the residues presented in the image.

More deeply in accuracy analysis for the output images and process replication (applying the algorithm for more than image) reveled that some characters are in similitude with the qualities of some objects in the output image of the additional aperture. To avoid wrong detection of defects and the confuse of these two defects, the length parameter was employed to distinguish between them, in the sense that the length of the object (residues) must not exceed than one third of the original image, otherwise, the object is not being residues.

3.4.3.1. Flowchart and the code of Residues defect

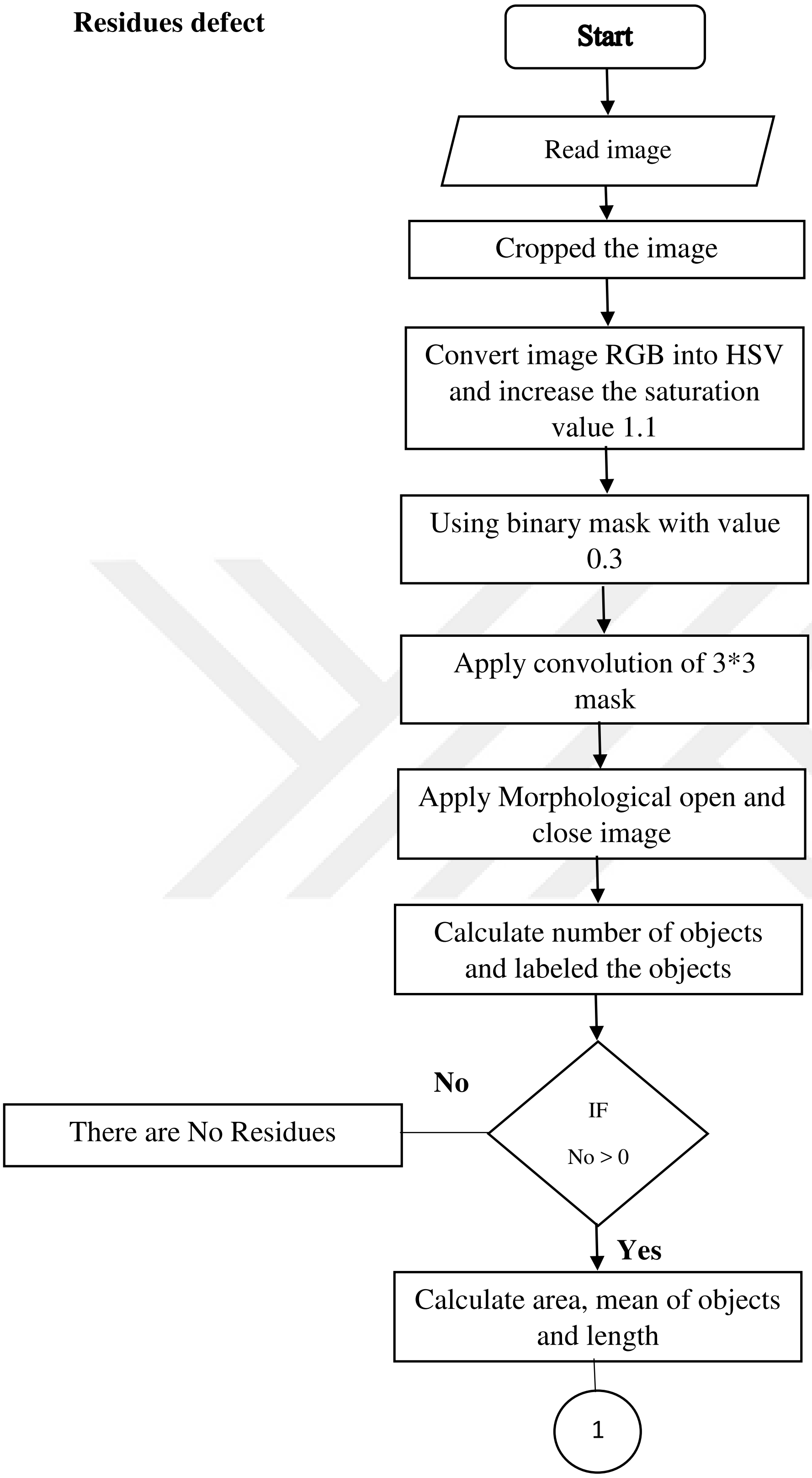

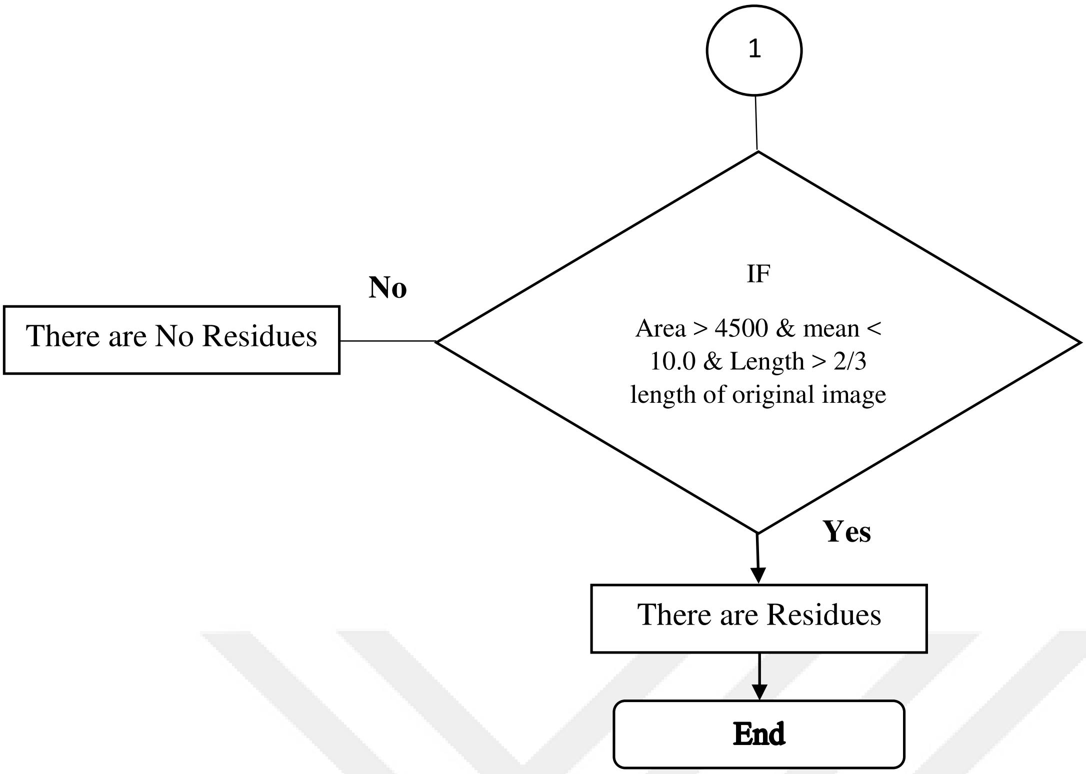

Flowchart 3 Residues detect algorithm

The code of Residues

```
function R  = Resdet( im )
rgb=im;
rect=[0 40 630 570];
I2 = imcrop(rgb,rect);
A=I2(1:180,:,:);
B=I2(180+1:end,:,:);
B1=imcrop(B,[11 0 630 300]);
HSV = rgb2hsv(B1);
HSV(:, :, 2) = HSV(:, :, 2) *1.1;
HSV(HSV > 1) = 1;
RGB = hsv2rgb(HSV);
H = rgb2hsv(RGB);
h = H(:, :, 1);
rgb = H(:, :, 2);
v = H(:, :, 3);
threshold = mean(rgb(:));
```

```
binaryMask = rgb > 0.1 * 3;
imageSize = size(binaryMask);
ci = [-40, 350, 170];
[xx,yy] = ndgrid((1:imageSize(1))-ci(1),(1:imageSize(2))-ci(2));
mask = double((xx.^2 + yy.^2)>ci(3)^2);
croppedImage = double(zeros(size(binaryMask)));
 croppedImage = binaryMesk.*mask;
  se = strel('disk',7);
closeBW = imopen(croppedImage,se);
  se = strel('disk',10);
  closeBW = imclose(closeBW,se);
BW2 = bwareaopen(closeBW, 180);
BW2=double(BW2);
  level=graythresh(BW2); bw=im2bw(BW2,level);
 [labeled,numObjects]=bwlabel(bw,4);
info=regionprops(labeled,'all');
 if numObjects>0
Extrema1=info(1).Extrema ;
  info(1).Area;
  Areas=cat(1,info.Area);
  mask=logical(closeBW);
red=immultiply(mask,B1(:,:,1));
g=immultiply(mask,B1(:,:,2));
b=immultiply(mask,B1(:,:,3));
im=cat(3,red,g,b);
 [m n k]=size(im);
I=reshape(im,m*n,3);
idx=find(mask);
[m n]= size(croppedImage);
  me=mean2(im);
  xx=0;
 No=numObjects;
  bigest_Area=info(1).Area;
for i=2:numObjects
```

```
if(bigest_Area<info(i).Area)
    bigest_Area=info(i).Area;
end
end
 in=find(cat(1,info.Area)==bigest_Area);
Extrema1=info(in).Extrema;
lenght=Extrema1(6,2)-Extrema1(1,2);
[m n K]=size(B1);
r=im(:,:,1);
 Gmean=mean2(r);
for i=1:No
 xx= xx+ info(i).Area;
 end
  if No>1
     if (xx >9500  && me <10.0 && lenght < m-70 )
         disp(sprintf('there are Residues' ));
 R=1;
     else
    disp(sprintf('there are  NO Residues'));
R=0;
      end
 else
     if (xx >200 &&Gmean>0.20 && me <3.65 && lenght < m-160 )
   disp(sprintf('there are Residues' ));
R=1;
else
   disp(sprintf('there are  NO Residues'));
R=0;
     end
end
else
   disp(sprintf('there are  NOo Residues'));
R=0;
end
```

3.4.4. Implementation of image segmentation algorithm

There are two aims of image processing application, image improving and analysis, for extraction specific information about the image, in order to enable the computer for understanding and interpretation of the studied image. One of the most interesting stages during image analysis is " image segmentation" which attracted workers to apply it widely. The goal of image segmentation is divide the image into number of un-interacted sects. In other words, isolate and define uniform sects from the image and ultimately identify their morphological properties.

Image containing fraction, characterized by presence of uniform sects of similar properties, as shown below in figure (3.20.). These sects are the fractions which were consider in this study as the objects, we intend to separate and analyze. Image segmentation techniques were used in fraction discovery, bounding detection which is one approach of segmentation techniques and is regarded as the extension of edge detection, was used also to easily discover of the objects that possess enough contrast in the background of the tested image. This is, however, the case of the fractions in such images where the objects in question is quite varied as compared to the background.

Figure 3.20. Capillary fraction

Contrasts may have detected by operator which estimate the image gradient. On the other hand, the image gradient could be estimated and applying the threshold to establish binary mask containing the object under study, by estimate the threshold automatically using Sobel operator. To create binary mask having the object (fraction) to be separated, Sobel operator was used again. After making the binary mask a high contrast lines appeared in the object. These lines (noise) effect obviously the clearance of the object by preventing the object boundaries lines to be seen clearly as illustrate in figure (3.21.). The abovementioned noise would be disappeared by employing linear structuring elements. Therefore, in this trial, this noise disappeared by using Vertical structuring elements followed by Horizontal structuring elements. Image was successfully separated, but some objects were found attached to the object boundary. These objects were eliminated by applying imclearborder function followed by smoothing process. Eroding the image was used twice respectively for more clearing appearance of the object (fraction). So, the output as shown in figure (3.22.) was clear enough object image that could be easy to study and extract its characters in order to distinguish the tested image from the other images free of these types of defects.

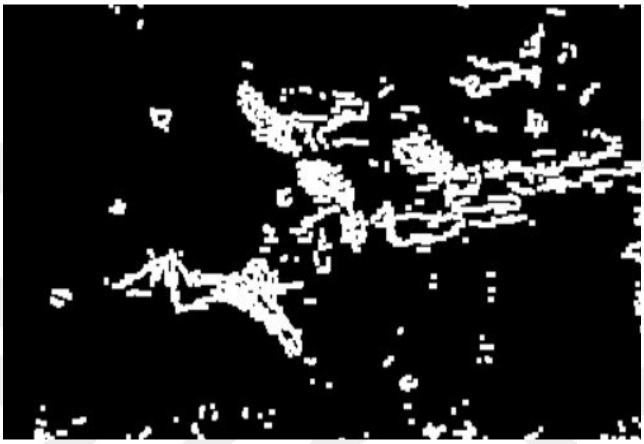

Figure 3.21. Capillary fraction with some noise

Figure 3.22. Capillary fraction without noise

The tested image may have more than one fraction (object) it was expected that the input image would have more than one interested region. That is why, the total area of the region was estimated and used as comparison element for discovering of the fractions.

The hardest challenge in this work having fractions, was almost equal to the area of some objects in the output images from the application of residues diagnosing algorithm.

As this work is a comprehensive project for all the studied defects, all necessary precaution must be taken to avoid any type of mistakes. Thus, it was necessary to find out other comparison element for isolation of these two types of defects. It was found, by more accurate analysis of the problem, that the object (residues) saturation values was higher than the values of the regions which is fraction. That is why, the region and the object were converted from RGB space to HSV space, beside estimating the means of pixels' value of the array (S) inside the object and these means were compared with the threshold. The big values reflect the residues while the small are fraction.

3.4.4.1. Flowchart and the code of

Capillary fraction defect

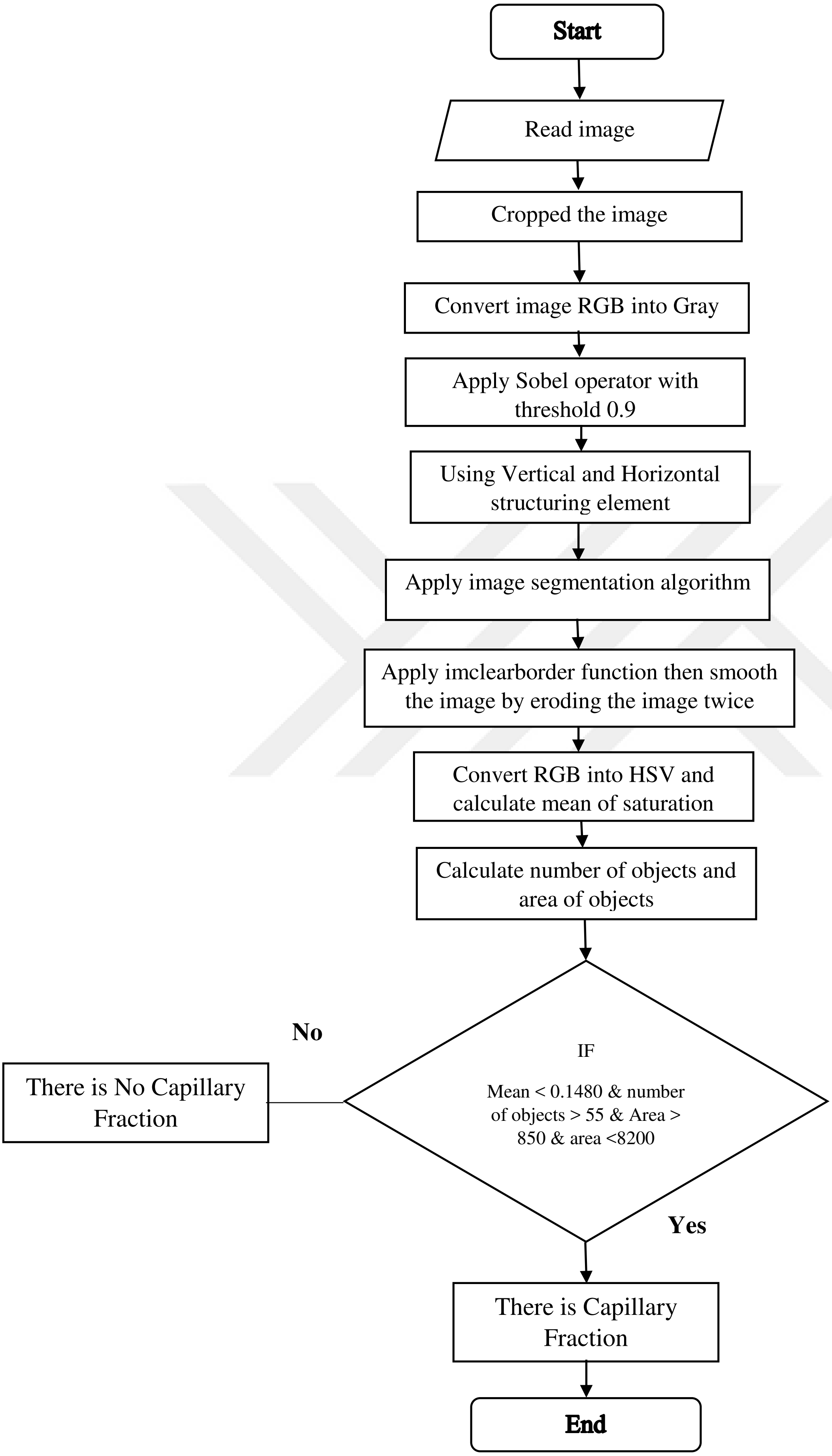

Flowchart 4 Capillary fraction detect algorithm

The code of Capillary fraction

```
function C = fractions_detect( im )
rgb=im;
rect=[0 40 630 570];
I2 = imcrop(rgb,rect);
A=I2(1:180,:,:);
B=I2(180+1:end,:,:);
A1=imcrop(A,[250 0 630 180]);
B1=imcrop(B,[11 0 430 250]);
I=rgb2gray(B1);
 [~, threshold] = edge(I, 'sobel');
Factor = 0.9;
BWs = edge(I,'sobel', threshold * Factor);
se90 = strel('line', 3, 90);
se0 = strel('line', 3, 0);
BWsdil = imdilate(BWs, [se90 se0]);
BWdfill = imfill(BWsdil, 'holes');
BWnobord = imclearborder(BWdfill, 4);
seD = strel('diamond',1);
BWfinal = imerode(BWnobord,seD);
  BWfinal = imerode(BWfinal,seD);
BW2 = bwareaopen(BWfinal,30);
hsi = rgb2hsv(im);
i=hsi(:,:,2);
m=mean2(i);
maxValue = max(i(:));
if m < 0.118
    w=1;
else
    w=0;
end
BW2=double(BW2);
  level=graythresh(BW2); bw=im2bw(BW2,level);
 [labeled,numObjects]=bwlabel(bw,4);
```

```
info=regionprops(labeled,'all');
if numObjects >0
 a=1 ;
  d=1;
 for t=1: numObjects
   AA=info(t).Area ;
   if (AA>10)
im1=(labeled==a);
 a=a+1 ;
mask=logical(im1);
red=immultiply(mask,B1(:,:,1));
g=immultiply(mask,B1(:,:,2));
b=immultiply(mask,B1(:,:,3));
im=cat(3,red,g,b) ;
 ip=1;
qq=0;
[m n k]=size (im);
for ii=1:m
    for jj=1:n
        if im(ii,jj)>1
            qq(ip)=im(ii,jj);
            ip=ip+1;
        end
    end
end
    pppp(d)=max(qq);
    pppn(d)=min(qq);
 meee(d)=mean2(qq);
 mean2(qq);
   md= median(qq) ;
 d=d+1;
end
 end
 u=mean2(meee) ;
```

```
 umax=mean2(pppp);
 umin=mean2(pppn);
 maxpp=max(pppp);
 minpp=min(pppn);
tdf=maxpp-minpp;
end
xx=0;
for i=1:numObjects
 xx= xx+ info(i).Area;

end
if(w==1 &&   numObjects < 40 && xx>1349 && xx<3200)
     disp('there are fraction');
if(u> 147 && tdf >67)
   C=1;

else
    C=0;
end
elseif (w==0   | numObjects>25 |  xx<1460  | xx>4000  )
disp('there are no fraction');
C=0;
else
       disp('there are fraction');
if(u> 147 && tdf >67)
C=1;
 else
    C=0;
 end
end
end
```

3.5. Flowchart of General Program

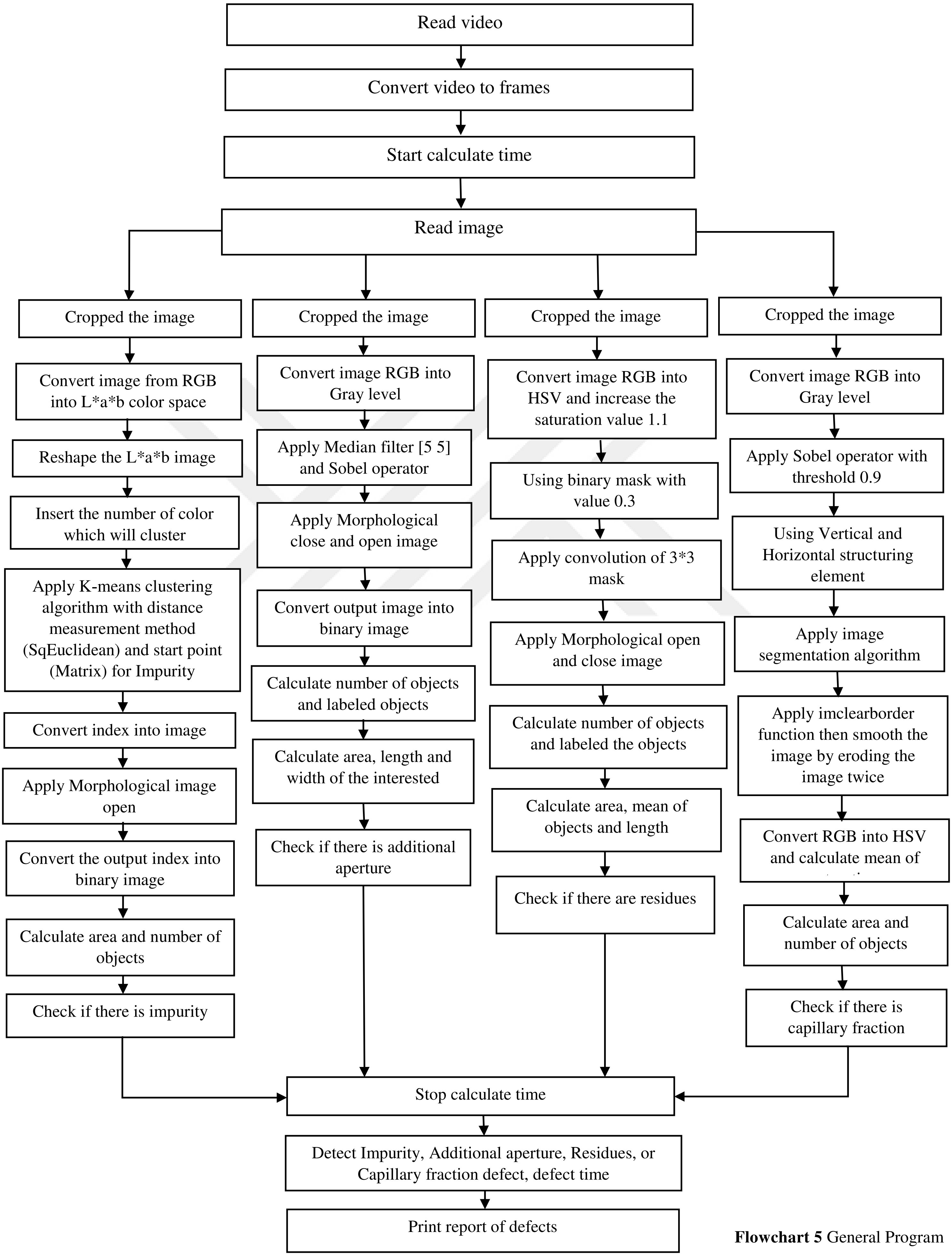

Flowchart 5 General Program

4. RESULTS AND DISCUSSION

4.1. Results

For simulation of the proposed work, MATLAB R2012a software was used in this study. This software quality makes it efficient and suitable for easy and accurate applying such algorithms. This program could analyze and represent giving data by processed it according to its datasets.

The accuracy and efficiency of the proposed algorithms were estimated through applying these algorithms on some datasets to obtain the accuracy desired via applying the following equations (4.1): -

$$Precision_{(i)} = \frac{\text{Correctly defects detected}_{(i)}}{\text{Total images tested containing defect}_{(i)}} * 100 \qquad (4.1)$$

Where, i= Impurities defect, Residues defect, Additional aperture defect and Capillary fraction defect.

4.1.1. Results of the defects (Impurity, Additional aperture, Residues and Capillary fraction) as an images

By apply the proposed algorithm, result was binary image included the background and the object. The data (results) obtained from the object analysis were used to detect the Impurities in the image under investigation. Table (4.1.) below show the application of the proposed algorithm on datasets depending upon evaluation of the algorithm via estimate its accuracy.

After the separation of the background from the part under study by applying the proposed algorithm for finding out the Additional aperture which is a line passing between regions of different properties (un-similar). Accuracy of the proposed work was estimated, in addition to estimate the error rate and shown in the table (4.1.).

After the steps of this proposed work for detecting the Residues defect, the output images were having different number of objects (Residues). Therefore, results of the accuracy percent of this work are presented in the table (4.1.).

Following the segmentation process and obtaining the interest region, this region was analyzed and its properties were identified. These properties were used for diagnosing the defect correctly (Capillary fraction). The algorithm was examined by applying it or datasets and estimating accuracy, and the results are shown in the table (4.1.):

Table 4.1. Accuracy for Impurity, Additional Aperture, Residues and Capillary fraction detect

Algorithm	Accuracy			
	Impurities	Additional Aperture	Residues	Capillary Fraction
Impurity detect Algorithm	**100 %**	13 %	8 %	0 %
Additional aperture Detect Algorithm	0 %	**100 %**	7.1 %	0 %
Residues detect Algorithm	0 %	0 %	**100 %**	0 %
Capillary fraction detect algorithm	0 %	0 %	0 %	**100 %**

4.1.2. Results of the defects (Impurity, Additional aperture, Residues and Capillary fraction) as a videos

The following figure (4.1.), show GUI (Graphic User Interface) program. Information can be inserted to the GUI of any given videos, and also can select the videos easily by choose them from a prepared list in the program. During the processing operation, the figures of defects can also be shown through click on the defects on the left side of the list. After the manipulation of the video, clicking on the publish button gives a report of the defects.

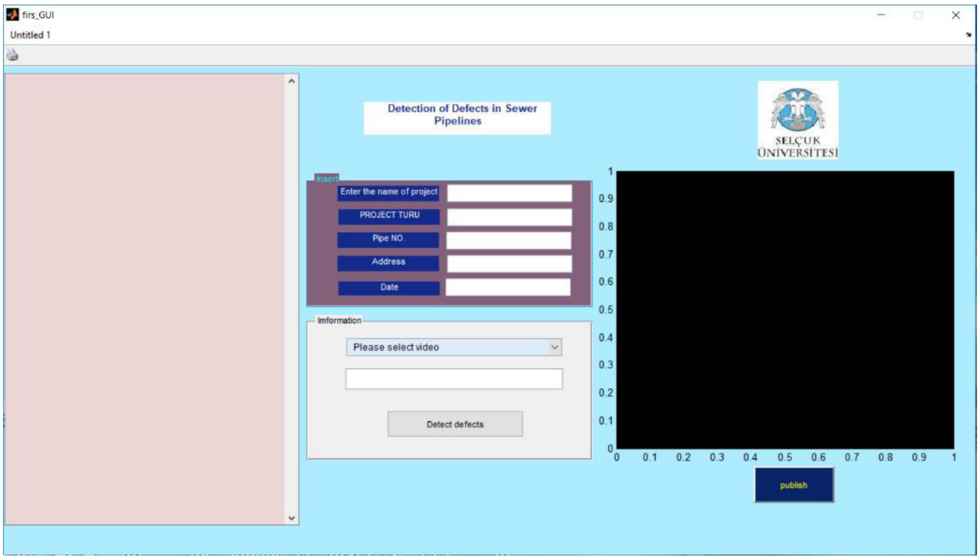

Figure 4.1. GUI of our program

Form a comparison point of the view between the process defect determination by man eye and the application of the outputs this study, it is very much obvious from the comparison results of two videos that there was a high percent of accuracy. In video number one (4.34 minutes) it was (96.42 %), the program found 27 defects in 4.51 minutes whereas, human test discovered 28 defects in 14.23 minutes. After the manipulation of the video, can click on any defect in the left side of the GUI to show the defect figure, as shown in the figure (4.2.).

Figure 4.2. After the manipulation of the video

It is worthy to mention here that this program gives the results as report on the Microsoft Excel by clicking on publish button (figure (4.3.)), while by the other method the results should be written by hand that my take longer time.

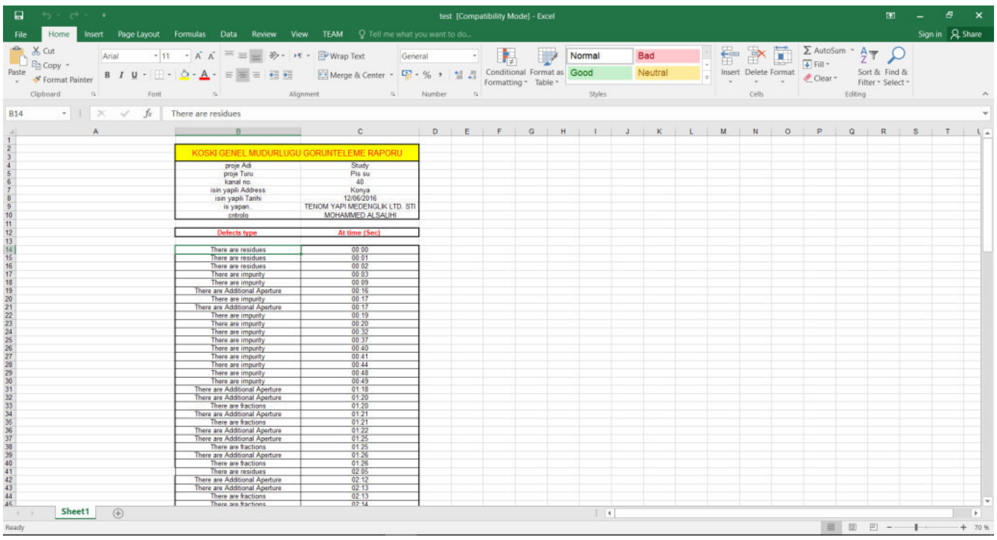

Figure 4.3. Our program report in Microsoft Excel.

Below a company report that have been forwarded to the municipal office and our program report after saved it:

KOSKI GENEL MUDURLUGU GORUNTELEME RAPORU	
Proje Adi	KOSKI YUNAK PIRIBEYLI KNZ INS
Proje Turu	Pis su
kanal NO.	40
isin yapildigi Adres	Konya / KOYICI 175
isin yapilis Tarihi	12.06.2016
isi yapan Firma Adi	TENOM YAPI MEDENGLIK LTD. STI
Kontrolu yapan	MOHAMMED ALSALIHI
Defects type	**At time (Sec)**
There are residues	00:00
There are residues	00:01
There are residues	00:02
There are impurity	00:03
There are impurity	00:09
There are Fractions OR Scratch	00:13
There are Additional Aperture	00:16
There are impurity	00:17
There are Additional Aperture	00:17
There are impurity	00:19
There are impurity	00:20
There are Fractions OR Scratch	00:23
There are Fractions OR Scratch	00:24
There are Fractions OR Scratch	00:25
There are Fractions OR Scratch	00:30
There are Fractions OR Scratch	00:31
There are impurity	00:32
There are Fractions OR Scratch	00:33
There are Fractions OR Scratch	00:35
There are Fractions OR Scratch	00:36
There are impurity	00:37
There are Fractions OR Scratch	00:38
There are Fractions OR Scratch	00:39

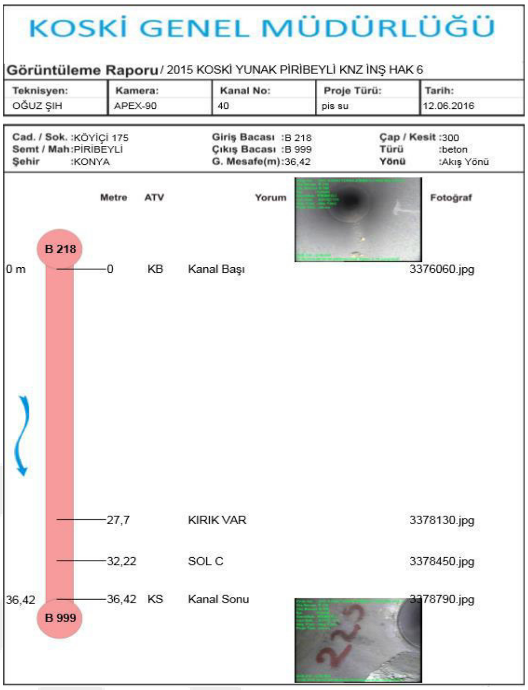

Our Program Report   Company Report

Number two, 7.53- minutes video was also compared. Results reflect that by human eye, 30 defects were identified in 18.36 minutes, while using our program, 29 defects were defected in 8.52 minutes as a report at the Microsoft Excel. This indicated that our program accuracy reached (96.66 %). After the manipulation of the video, the defect can show in the left side of GUI, figure (4.4.).

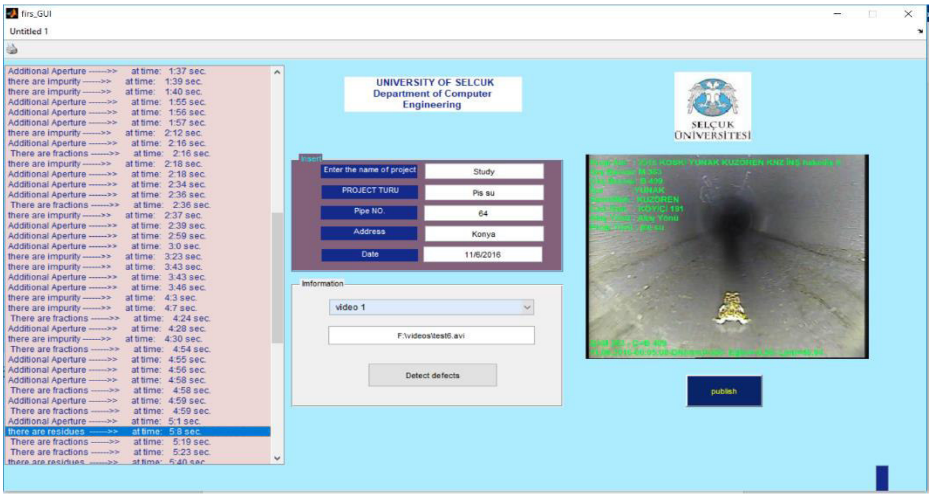

Figure 4.4. After the manipulation of the video

After process operation finshed, all kind of defects and the time given in as a report at the Microsoft Excel by clicking on publish button as shown in figure (4.5.).

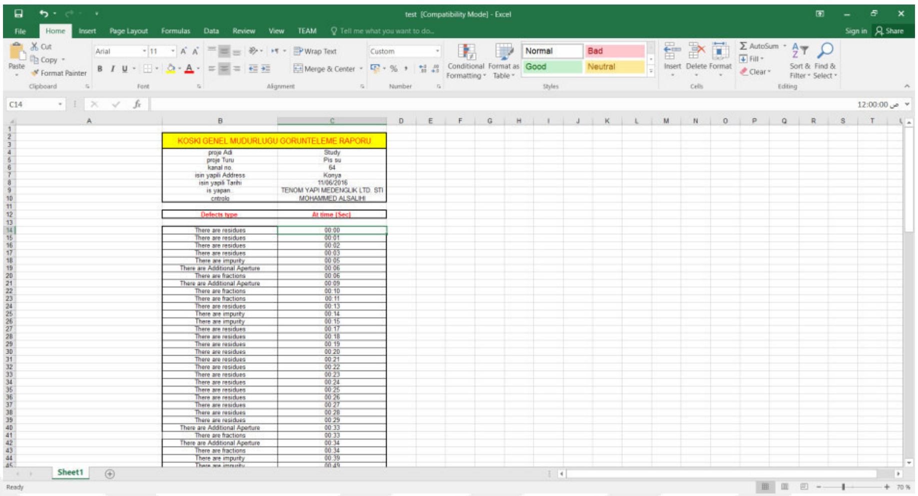

Figure 4.5. Our program report in Microsoft Excel

Below a company report that have been forwarded to the municipal office and our program after save it:

KOSKI GENEL MUDURLUGU GORUNTELEME RAPORU	
Proje Adi	Test 2
Proje Turu	Pis su
kanal NO.	64
isin yapildigi Adres	Konya
isin yapilis Tarihi	11.06.2016
isi yapan Firma Adi	TENOM YAPI MEDENGLIK LTD. STI
Kontrolu yapan	MOHAMMED ALSALIHI
Defects type	**At time (Sec)**
There are residues	00:00
There are residues	00:01
There are residues	00:02
There are residues	00:03
There are impurity	00:05
There are Additional Aperture	00:06
There are Fractions OR Scratch	00:06
There are Additional Aperture	00:09
There are Fractions OR Scratch	00:10
There are Fractions OR Scratch	00:11
There are residues	00:13
There are impurity	00:14
There are impurity	00:15
There are residues	00:17
There are residues	00:18
There are residues	00:19
There are residues	00:20
There are residues	00:21
There are residues	00:22
There are residues	00:23
There are residues	00:24
There are residues	00:25
There are residues	00:26

Program report

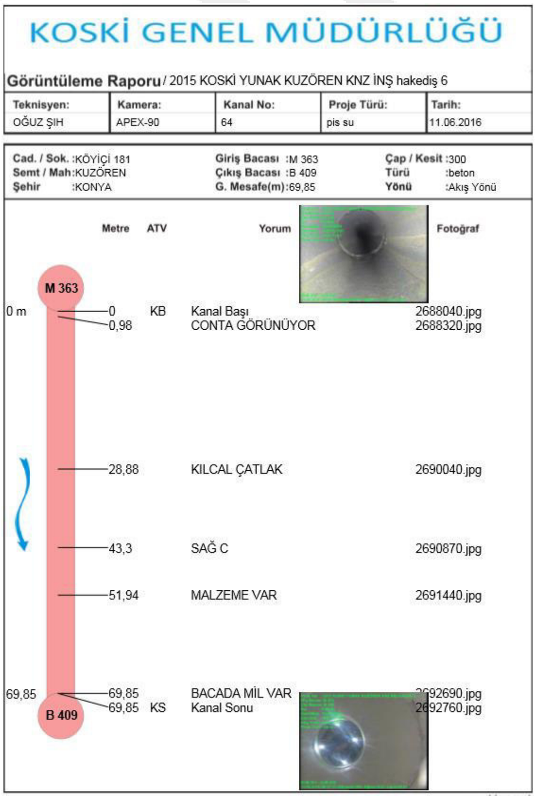

Company report

In the third video that took 3.59 minutes by the human eye 15 defects were seen in 8.28 minutes, while in 4.58 minutes in our technology 15 defects were determined. Therefore, the error is 0 %. After the manipulation of the video, the defect can show in the left side of GUI, figure (4.6.).

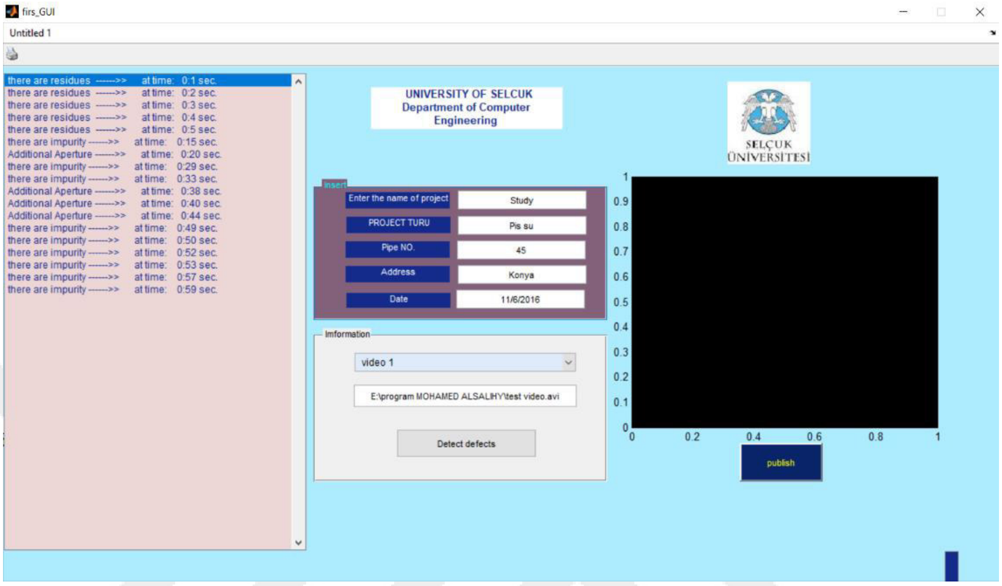

Figure 4.6. After the manipulation of the video

After process operation finshed, all kind of defects and the time given in as a report at the Microsoft Excel by clicking on publish button as shown in figure (4.7.).

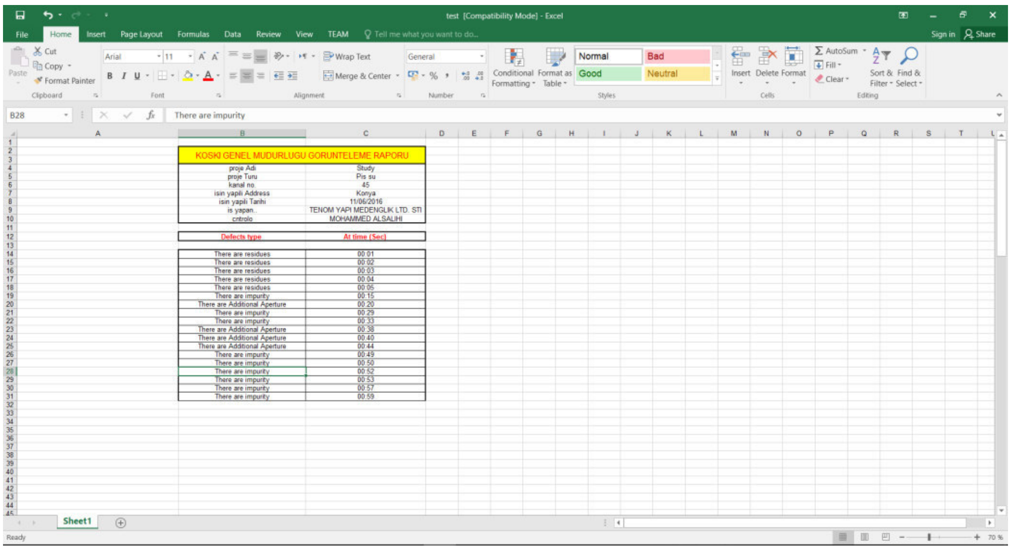

Figure 4.7. Our program report in Microsoft Excel

Below a company report that have been forwarded to the municipal office and our program after save it:

KOSKI GENEL MUDURLUGU GORUNTELEME RAPORU	
proje Adi	KOSKYUNAK KUZOREN KNZ
proje Turu	Pis su
kanal no.	45
isin yapili Address	Konya\KUZOREN
isin yapili Tarihi	11.06.2016
is yapan..	TENOM YAPI MEDENGLIK LTD. STI
cntrolo	OGUZSIH

Defects type	At time (Sec)
There are Residues	00:02
There are Fractions or Scratch	00:05
There are Additional Aperture	00:12
There are Fractions or Scratch	00:15
There are Fractions or Scratch	00:24
There are Additional Aperture	00:25
There are Additional Aperture	00:29
There are Fractions or Scratch	00:37
There are Impurity	00:40
There are Fractions or Scratch	00:41
There are Additional Aperture	00:49
There are Fractions or Scratch	00:56
There are Fractions or Scratch	00:57
There are Fractions or Scratch	01:00
There are Fractions or Scratch	01:03
There are Fractions or Scratch	01:04
There are Fractions or Scratch	01:09
There are Fractions or Scratch	01:11
There are Fractions or Scratch	01:13
There are Fractions or Scratch	01:14
There are Fractions or Scratch	01:16
There are Fractions or Scratch	01:17
There are Fractions or Scratch	01:19

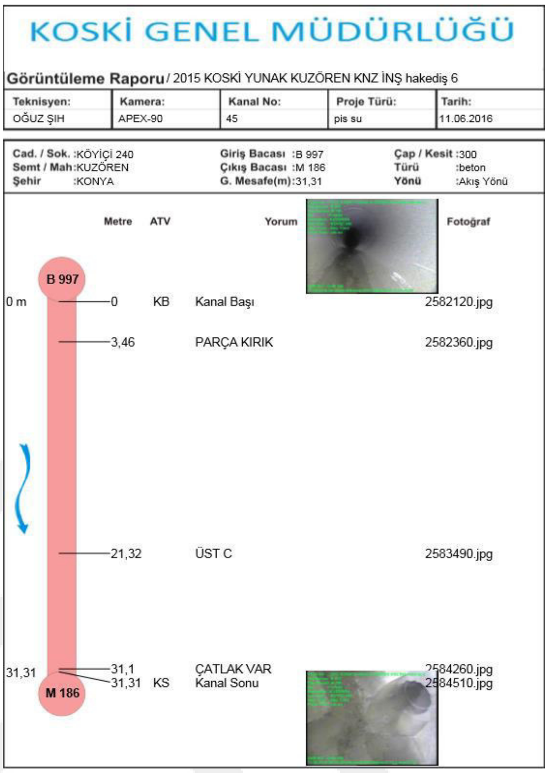

Program report   Company report

The error appeared in this study was probably due to some factors such as over illumination that may cause wrong identification, unitability of the camera on the robot while recording the videos, indistinct resulting images, wrong angle of picturing and other cases out of our control.

4.2. Discussion

The analysis of datum presented in tables (4.1.), replay that application of Impurity detection algorithm on images inputs having Impurity detect, can resulted a 100 % accuracy. In addition, it gives a reliable result when applied on fraction containing images with 0 % error. But when this algorithm applied on images inputs having Additional aperture, a low percent error may produce, because, the Additional aperture images have the same characters of the Impurities images, so, the algorithm used to diagnose Impurity may give some error when applied on additional aperture images.

The observed error percent in diagnoses the images having Residues as Impurities, was due to both Residues and Impurities have the same color (as have already been mentioned above), so, the Impurities were separated on the basis of the color, that is why the applied algorithm yielded wrong diagnosis (the image diagnosed as Impurities) when used on residues containing images.

The results regarding Additional aperture algorithm, show that there is a small error percentage when applied on residues containing images, that would be attributed to the presence of some images possess large area of the Residues. When these images were manipulated, the object was fused or integrated by the program and collectively formed single object in Additional aperture form, when analyzed and their characters were obtained, we found that it was Additional aperture.

Results reflect also the algorithms of Residues diagnosis and Capillary fraction detect, were very efficient and accurate as much as 100 % with 0% error. The reason was these algorithms characterized with very efficient analysis and identification ability, beside extracting input images qualities accurately as well.

5. CONCLUSION AND RECOMMENDATION

5.1. Conclusion

From the outstanding results of this study, the following conclusions can be extracted:

- Employing of K-means clustering technique in detecting of sub ground non-metal sewer pipelines Impurities, resulted in good and reliable results as compared to the other techniques used in this investigation.
- Edge detection technique by estimating area (pixels numbers), length and width gave swift clear and good detection for the Additional aperture.
- As for the image containing "Residues" as object, the HSV color space was employed after its conversion from RGB color space, reveal that the defect in question (i.e. Residues) was of high level of saturation, this lead (by estimate object characters) to easy discover the defect swiftly.
- Image separation technique was applicable in fraction discovery, by estimating the threshold automatically using Sobel operator to create binary mask having the object (Capillary fraction) to be separated. Then, by extracting its characters we were able to distinguish the tested image form the other image free of these types of defects.

5.2. Future Proposed Recommendation

For obtaining an efficient and accurate recognition for all types of non-metal sewer system defect through diagnosis their qualities by one of the recognition algorithm, we recommend to employ artificial intelligence techniques in this field of engineering work as non-metal sewer systems.

REFERENCES

Allouche, E. N. and Freure, P., 2002, Management and maintenance practices of storm and sanitary sewers in Canadian municipalities, Institute for Catastrophic Loss Reduction, p.

Bilmes, J. A., 2006, What HMMs can do, *IEICE TRANSACTIONS on Information and Systems*, 89 (3), 869-891.

Bora, D. J. and Gupta, A. K., 2014, A new approach towards clustering based color image segmentation, *International Journal of Computer Applications*, 107 (12).

Bora, D. J., Gupta, A. K. and Khan, F. A., 2015, Comparing the performance of L* A* B* and HSV color spaces with respect to color image segmentation, *arXiv preprint arXiv:1506.01472*.

Bora, M., Jyoti, D., Gupta, D. and Kumar, A., 2014, Effect of different distance measures on the performance of K-means algorithm: an experimental study in Matlab, *arXiv preprint arXiv:1405.7471*.

Buchsbaum, G., 1980, An analytical derivation of visual nonlinearity, *IEEE Transactions on biomedical engineering* (5), 237-242.

Daher, S., 2015, Defect-based Condition Assessment Model and Protocol of Sewer Pipelines, *Concordia University*.

Daniels, D. J., 2005, Ground penetrating radar, Wiley Online Library, p.

Dugad, R. and Desai, U. B., 1996, A tutorial on hidden Markov models, *Signal Processing and Artifical Neural Networks Laboratory, Dept of Electrical Engineering, Indian Institute of Technology, Bombay Technical Report No.: SPANN-96.1*.

Duran, O., Althoefer, K. and Seneviratne, L. D., 2002, Automated sewer pipe inspection through image processing, *Robotics and Automation, 2002. Proceedings. ICRA'02. IEEE International Conference on*, 2551-2556.

Feeney, C., Thayer, S., Bonomo, M. and Martel, K., 2009, White paper on condition assessment of wastewater collection systems, *National Risk Management Research Laboratory*.

Feng, Q., Li, R., Nie, B., Liu, S., Zhao, L. and Zhang, H., 2016, Literature Review: Theory and Application of In-Line Inspection Technologies for Oil and Gas Pipeline Girth Weld Defection, *Sensors*, 17 (1), 50.

Fu, W., 2014, Feature Extraction in Edge Detection using Genetic Programming.

Gao, J., Chen, K., Wu, P., Chen, L. and Lin, P., 2017, Leakage detection of pipeline based on weighted-permutation entropy, *Control And Decision Conference (CCDC), 2017 29th Chinese*, 2820-2823.

Gupta, S. and Kaur, Y., 2014, Review of different local and global contrast enhancement techniques for a digital image, *Int J Comp Appl*, 100 (18), 17625-18384.

Hao, T., Rogers, C., Metje, N., Chapman, D., Muggleton, J., Foo, K., Wang, P., Pennock, S. R., Atkins, P. and Swingler, S., 2012, Condition assessment of the buried utility service infrastructure, *Tunnelling and Underground Space Technology*, 28, 331-344.

Hastie, T., Tibshirani, R. and Friedman, J., 2002, The Elements of Statistical Learning: Data Mining, Inference, and Prediction, *Biometrics*.

Jain, A. K., Duin, R. P. W. and Mao, J., 2000, Statistical pattern recognition: A review, *IEEE Transactions on pattern analysis and machine intelligence*, 22 (1), 4-37.

Jameel, S. K. and Manza, R. R., 2012, Color image segmentation using Wavelet', *IJAIS*, 1 (6), 1-4.

Jensen, J. A. and Svendsen, N. B., 1992, Calculation of pressure fields from arbitrarily shaped, apodized, and excited ultrasound transducers, *IEEE transactions on ultrasonics, ferroelectrics, and frequency control*, 39 (2), 262-267.

Kawaguchi, Y., Yoshida, I., Kurumatani, H., Kikuta, T. and Yamada, Y., 1995, Internal pipe inspection robot, *Robotics and Automation, 1995. Proceedings., 1995 IEEE International Conference on*, 857-862.

Maeyama, S., Ohya, A. and Yuta, S. i., 1995, Non-stop outdoor navigation of a mobile robot-Retroactive positioning data fusion with a time consuming sensor system, *Intelligent Robots and Systems 95.'Human Robot Interaction and Cooperative Robots', Proceedings. 1995 IEEE/RSJ International Conference on*, 130-135.

Magori, V., 1989, Signal processing for smart ultrasonic sensors, *CompEuro'89.,'VLSI and Computer Peripherals. VLSI and Microelectronic Applications in Intelligent Peripherals and their Interconnection Networks', Proceedings.*, 3/21-23/26.

Maini, R. and Aggarwal, H., 2009, Study and comparison of various image edge detection techniques, *International journal of image processing (IJIP)*, 3 (1), 1-11.

Marsland, S., Nehmzow, U. and Shapiro, J., 2005, On-line novelty detection for autonomous mobile robots, *Robotics and Autonomous Systems*, 51 (2), 191-206.

Mittal, U. and Anand, S., 2013, Modified watershed segmentation with denoising of medical images, *International Journal of Innovative Research in Science, Engineering and Technology*, 2 (4), 982-987.

Morales-González, A., Acosta-Mendoza, N., Gago-Alonso, A., García-Reyes, E. B. and Medina-Pagola, J. E., 2014, A new proposal for graph-based image classification using frequent approximate subgraphs, *Pattern Recognition*, 47 (1), 169-177.

Moreno, R., Puig, D., Julià, C. and Garcia, M. A., 2009, A new methodology for evaluation of edge detectors, *Image Processing (ICIP), 2009 16th IEEE International Conference on*, 2157-2160.

Morissette, L. and Chartier, S., 2013, The k-means clustering technique: General considerations and implementation in Mathematica, *Tutorials in Quantitative Methods for Psychology*, 9 (1), 15-24.

Mustafa, Z. A., Abrahim, B. A. and Kadah, Y. M., 2012, K11. Modified Hybrid Median filter for image denoising, *Radio Science Conference (NRSC), 2012 29th National*, 705-712.

Nassiraei, A. A., Kawamura, Y., Ahrary, A., Mikuriya, Y. and Ishii, K., 2007, Concept and design of a fully autonomous sewer pipe inspection mobile robot" kantaro", *Robotics and Automation, 2007 IEEE International Conference on*, 136-143.

Ohtani, K. and Baba, M., 2004, Shape recognition by network configuration of ultrasonic sensor array and CCD image sensors, *Circuits and Systems, 2004. MWSCAS'04. The 2004 47th Midwest Symposium on*, II-II.

Othman, Z., Haron, H., Kadir, M. R. A. and Rafiq, M., 2009, Comparison of Canny and Sobel Edge Detection in MRI Images, *Computer Science, Biomechanics & Tissue Engineering Group, and Information System*, 133-136.

Paletta, L. and Pinz, A., 2000, Active object recognition by view integration and reinforcement learning, *Robotics and Autonomous Systems*, 31 (1), 71-86.

ping Tian, D., 2013, A review on image feature extraction and representation techniques, *International Journal of Multimedia and Ubiquitous Engineering*, 8 (4), 385-396.

Poobathy, D. and Chezian, R. M., 2014, Edge detection operators: Peak signal to noise ratio based comparison, *International Journal of Image, Graphics and Signal Processing*, 6 (10), 55.

Qian, J., Yang, J. and Gao, G., 2013, Discriminative histograms of local dominant orientation (D-HLDO) for biometric image feature extraction, *Pattern Recognition*, 46 (10), 2724-2739.

Qin, Y. and Bao, N.-K., 1995, Thermographic nondestructuve testing (NDT) technique for delaminated defects in composite structures, *SPIE's 1995 Symposium on OE/Aerospace Sensing and Dual Use Photonics*, 219-223.

Robertson, P. and Schonhut, J., 1999, Color in computer graphics, *IEEE Computer Graphics and Applications*, 19 (4), 18-19.

Safizadeh, M. and Azizzadeh, T., 2012, Automated detection of inner surface defects in pipes using image processing algorithms.

Saraf, Y., 2006, Algorithms for image segmentation, *Birla Institute of Technology and Science*.

Seyyedi, S. A. and Ivanov, N., 2014, Statistical Image Classification for Image Steganographic Techniques, *International Journal of Image, Graphics and Signal Processing*, 6 (8), 19.

Singh, A., Yadav, A. and Rana, A., 2013, K-means with Three different Distance Metrics, *International Journal of Computer Applications*, 67 (10).

Sinha, S. K., 2000, Automated underground pipe inspection using a unified image processing and artificial intelligence methodology.

Sobel, I., 2014, History and definition of the sobel operator, *Retrieved from the World Wide Web*.

Steinbach, M., Karypis, G. and Kumar, V., 2000, A comparison of document clustering techniques, *KDD workshop on text mining*, 525-526.

Swain, M. J. and Ballard, D. H., 1991, Color indexing, *International journal of computer vision*, 7 (1), 11-32.

Wandell, B. A., 1995, Foundations of vision, Sinauer Associates, p.

Xiao, K., Liang, A. L., Guan, H. B. and Hassanien, A. E., 2013, Extraction and application of deformation-based feature in medical images, *Neurocomputing*, 120, 177-184.

Xue-Fei, W. and Hua, B., 2009, Automated assessment of buried pipeline defects by image processing, *Intelligent Computing and Intelligent Systems, 2009. ICIS 2009. IEEE International Conference on*, 583-587.

Yang, M.-D. and Su, T.-C., 2008, Automated diagnosis of sewer pipe defects based on machine learning approaches, *Expert Systems with Applications*, 35 (3), 1327-1337.

ÖZGEÇMİŞ (C.V)

KİŞİSEL BİLGİLER

Adı Soyadı	**:**	Mohammed Qays Jameel AL-SALIHI
Uyruğu	**:**	IRAK
Doğum Yeri ve Tarihi	**:**	BAGDAD 21/4/1991
Telefon	**:**	05315072491
e-mail	**:**	Alsalihy_Mohamed@yahoo.com

EĞİTİM

Derece		**Adı, İlçe, İl**	**Bitirme Yılı**
Lise	:	Al-Maarif , Baghdad	2008-2009
Üniversite	:	Diglla University College	2012-2013

İŞ DENEYİMLERİ

Yıl	**Kurum**	**Görevi**
2013	**Itisaluna for calling-Baghdad/ Iraq**	**Team leader in the call center**
2015	**Exchange company-Baghdad/ Iraq**	**Accountant**

UZMANLIK ALANI: Computer Engineering

YABANCI DİLLER: English-Turkish

BELİRTMEK İSTEĞİNİZ DİĞER ÖZELLİKLER: Reading, Technology and Sport

YAYINLAR: Alsalihi, M.Q.J. and Selek, M., 2017, " *Determination of Additional Aperture in Non-Metal Sewer Pipes by Image Processing*", Communications on Applied Electronics (CAE), New York, USA vol.7, no. 6, pp 8-11 September 2017.